BIOGEOCHEMICAL AND ECOLOGICAL RESEARCH AT THE PORCUPINE ABYSSAL PLAIN

HA Ruhl*, SE Hartman, &
RS Lampitt *et al.*
National Oceanography Centre
h.ruhl@noc.ac.uk

« Time-series analysis in Marine science and applications for industry »
Conference in Logonna-Daoulas, France, 17-22 sept. 2012

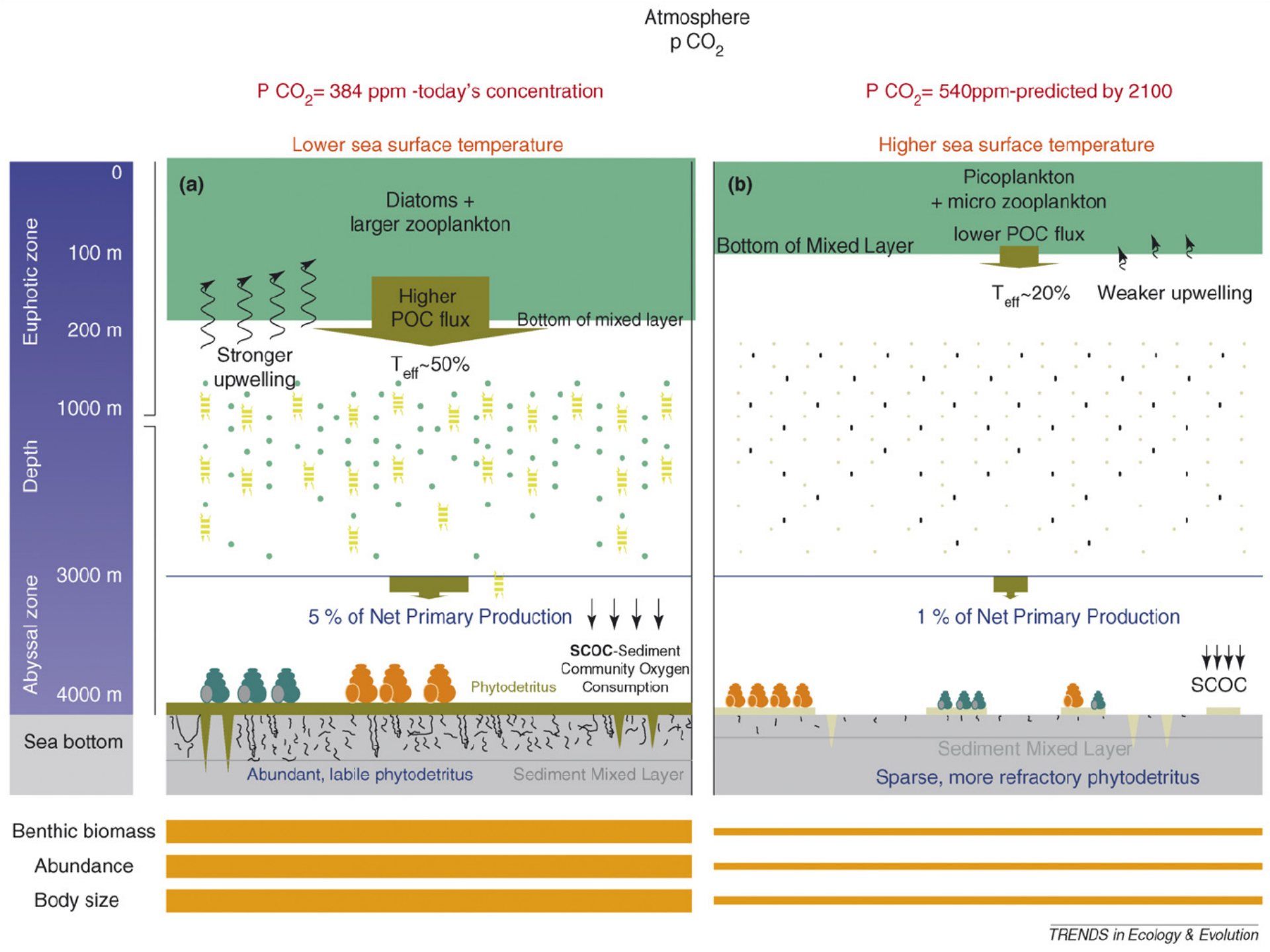
Atmosphere
p CO2
P CO2= 384 ppm -today's concentration
P CO2= 540ppm-predicted by 2100
Lower sea surface temperature
Higher sea surface temperature
0
Euphotic zone
100 m
200 m
Depth
1000 m
3000 m
Abyssal zone
4000 m
Sea bottom
(a)
Diatoms +
larger zooplankton
Higher
POC flux
Bottom of mixed layer
Stronger
upwelling
Teff~50%
5 % of Net Primary Production
SCOC-Sediment
Community Oxygen
Consumption
Phytodetritus
Abundant, labile phytodetritus
Sediment Mixed Layer
(b)
Picoplankton
+ micro zooplankton
Bottom of Mixed Layer
lower POC flux
Teff~20%
Weaker upwelling
1 % of Net Primary Production
SCOC
Sediment Mixed Layer
Sparse, more refractory phytodetritus
Benthic biomass
Abundance
Body size

Outline

- The setting at Porcupine Abyssal Plain
- Selected time series measurements
- Biophysical interactions
- PP and CO2 uptake
- Transfer of C into the deep ocean
- Seafloor life and the fate of C
- Future directions

Observatories in Europe

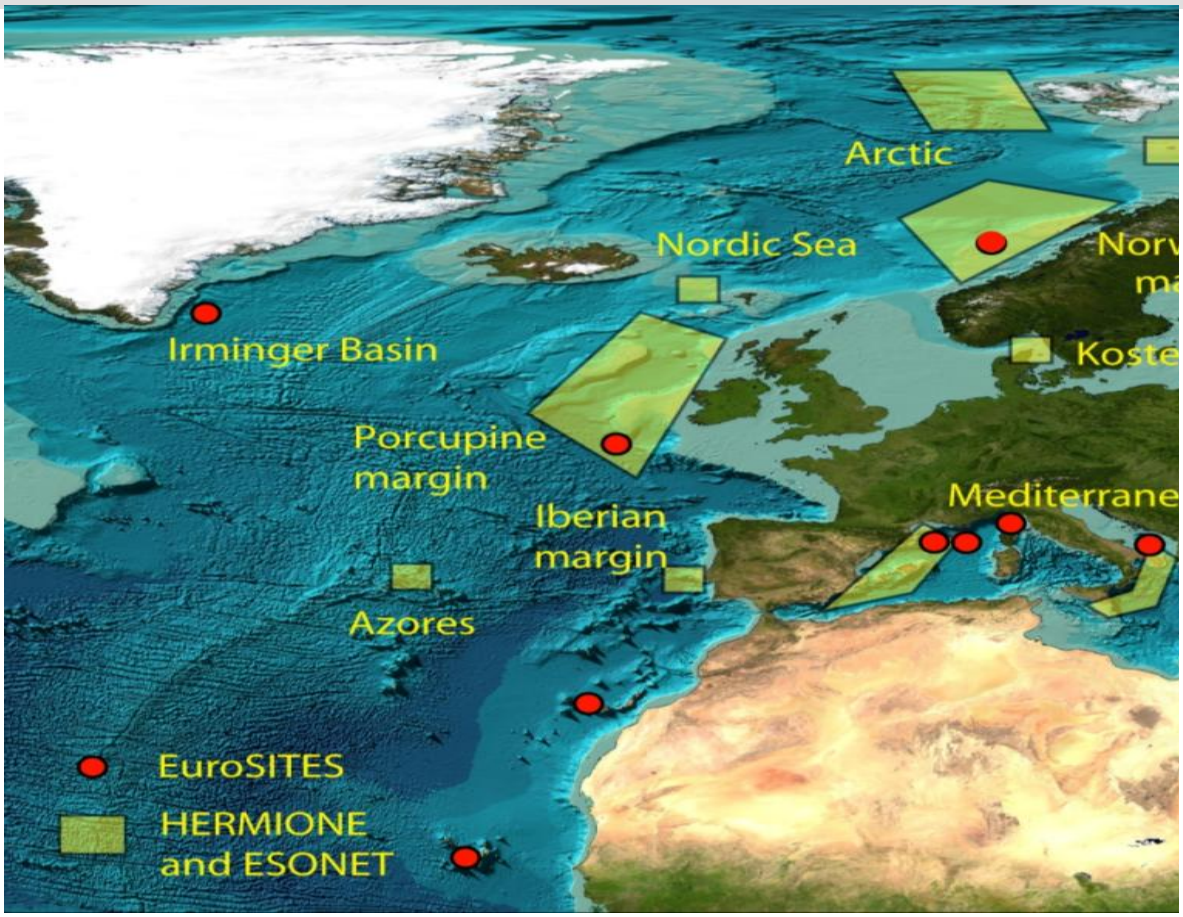

EuroSITES European Ocean Observatory Network

ESONET NOE

european multidisciplinary seafloor observatory emso

- NOC operates an observatory @ Porcupine Abyssal Plain.

Porcupine Abyssal Plain (PAP) - SO

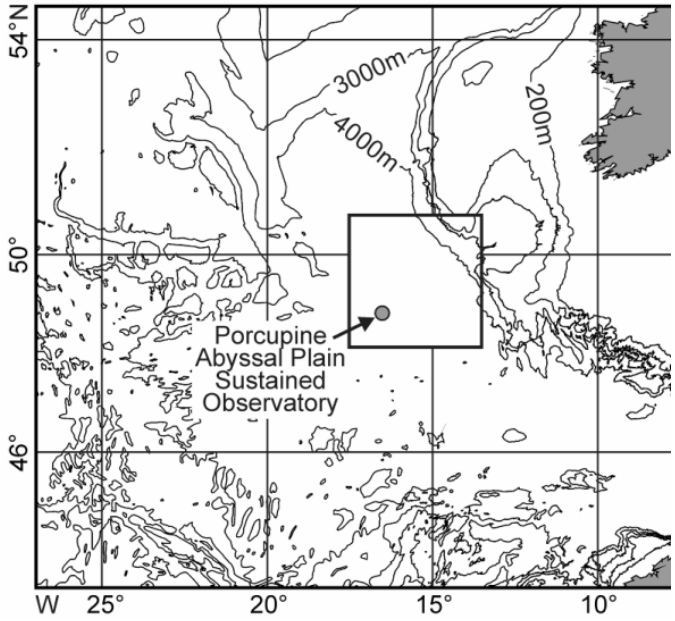

- Research @ ~4,850m depth in NE Atlantic since1989
- Evidence suggests POC flux at the site has links to the NAO & surface export flux
- Located in transition zone where MLD has dynamic links to PP and NAO variation
- UK contribution to OceanSITES and GOOS
- Major European open ocean observatory delivering real-time data, ‘pre-operational’ use
- Collaboration with MetOffice and many others

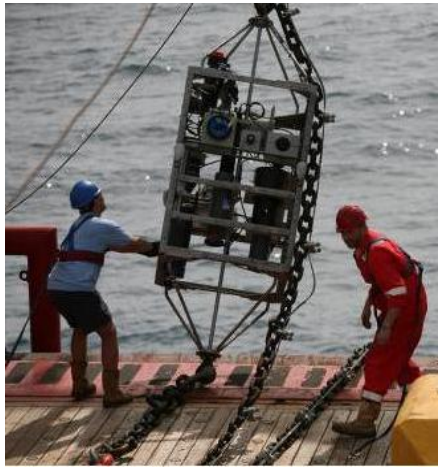

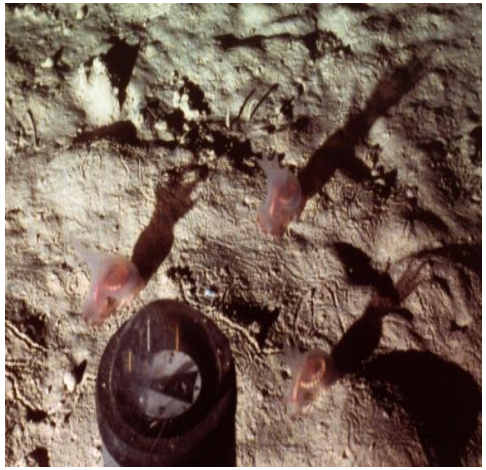

The PAP setting

North Atlantic Oscillation

Positive Phase

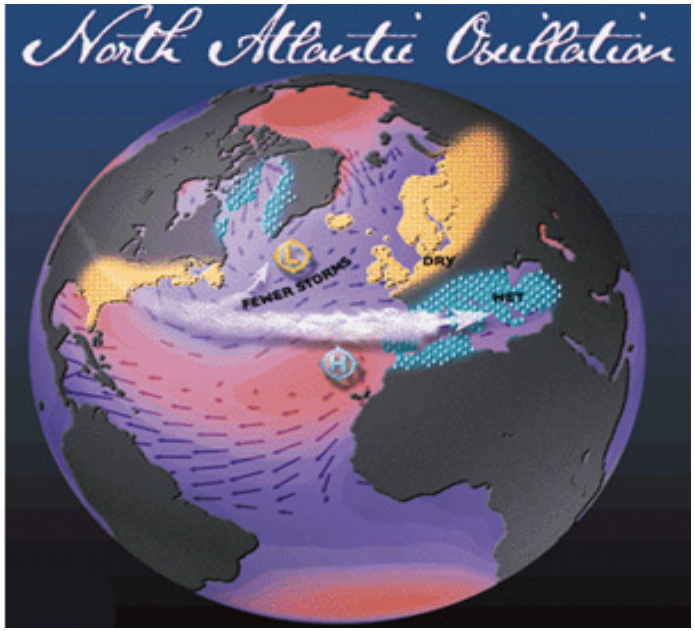

Negative Phase

The PAP setting

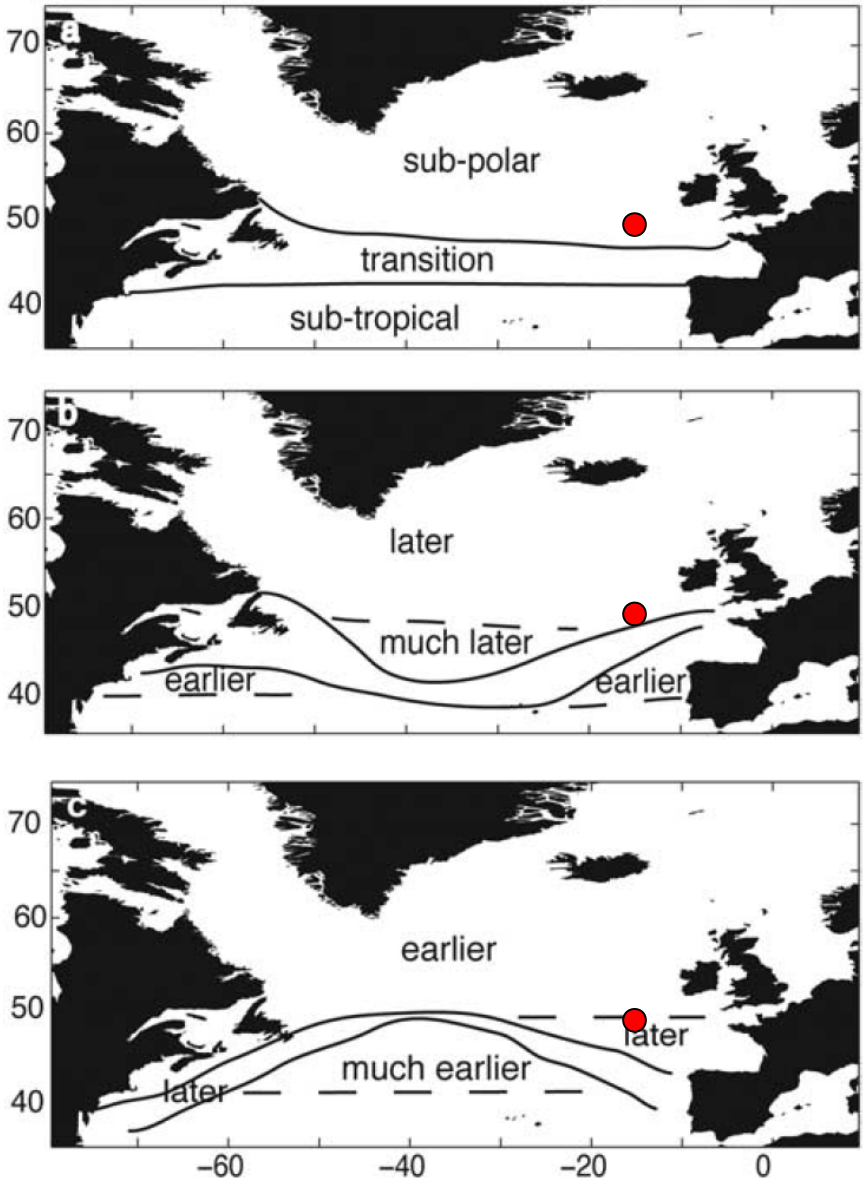

Figure 8. Sketch of the locations of the three bloom regions under (a) mean conditions, (b) in a positive NAO phase, and (c) in a negative NAO phase (dashed line marks position of transition region under mean conditions). The nature of the response in bloom timing is marked.

Henson et al. (2009), JGR

The PAP setting

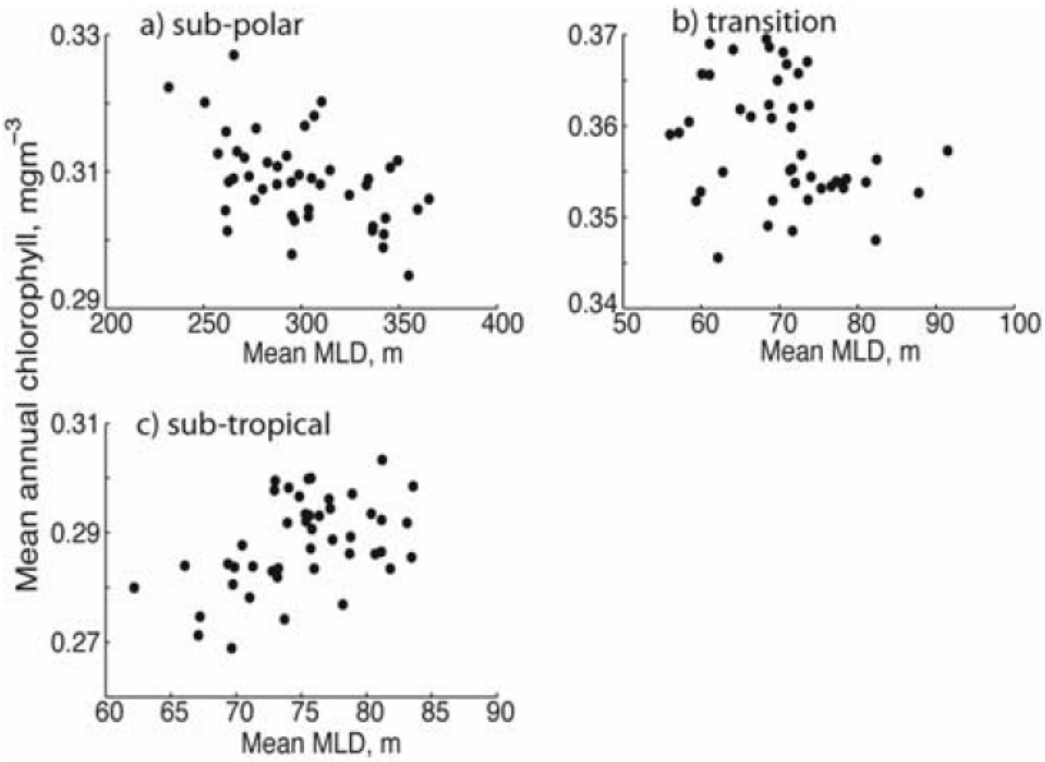

Figure 9. Mean annual modeled chlorophyll plotted as a function of mean annual MLD for the (a) subpolar, (b) transition, and (c) subtropical regions. Linear correlation coefficients are −0.48 ($p < 0.05$) and 0.49 ($p < 0.05$) for the subpolar and subtropical regions, respectively. Correlation coefficient for the transition region is not statistically significant.

Henson et al. (2009), JGR

PAP1
TO SERVICE
JC062

1271M OF 48mm PENDANT (138M OF 8 STRAND POLYPROPYLENE SPLICED IN TO 1135M OF 8 STRAND EUROFLEX)

4M OF 38mm CHAIN +
22M OF 32mm CHAIN

SENSOR FRAME

SWIVEL + 1.5M
OF 32mm CHAIN

MOORING BELOW THIS POINT REMAINED OUTBOARD OF VESSEL AND WAS NOT RECOVERED AND/OR INSPECTED

1.5M OF 38mm CHAIN

SUBSURFACE FLOAT

SWIVEL + 1.5M
OF 38mm CHAIN

1000M

1000M

4 X 1000M OF
8 STRAND
POLYPROPYLENE

1000M

ACOUSTIC
RELEASE

SN 1139
ARM 0827
REL 0855

1000M

TRIANGULATED
POSITION
48' 59.592 N
16' 22.168 W

20M OF 38mm CHAIN

3T SINKER

PAP 3
Deployed JC062
27/7/2011
48°59.382' N
16°29.585' W

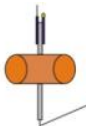

1 GLASS SPHERE

15m 16mm RECOVERY LINE

BILLINGS FLOAT WITH
XENON LIGHT s/n X03-076

5M ½"CHAIN

15m 20mm POLYPROP

12 GLASS SPHERES

SWIVEL

50m 10mm POLYESTER

3x 1m ¼" WIRE BRIDLE CONNECTED TO 3m ¼" WIRE

SEDIMENT TRAP
1800m from seabed

McLane Parflux 21way
s/n ML12432-02

3x 1m 3/8" CHAIN BRIDLE

RCM11 s/n 524

50m 10mm POLYESTER

SBE37IMP s/n 4460

3x 1m ¼" WIRE BRIDLE CONNECTED TO 3m ¼" WIRE

SEDIMENT TRAP
1750m from seabed

McLane Parflux 13way
s/n 532

3x 1m 3/8" CHAIN BRIDLE

1600m 10mm POLYESTER
(500 + 500 + 500 + 100)

10 GLASS SPHERES

SWIVEL

50m 10mm POLYESTER

3x 1m ¼" WIRE BRIDLE CONNECTED TO 3m ¼" WIRE

SEDIMENT TRAP
100m from seabed

McLane Parflux 21way
s/n ML12432-06

3x 1m 3/8" CHAIN BRIDLE

RCM11 s/n 425

50m 10mm POLYESTER

2 GLASS SPHERES

1m ½"CHAIN

Rt661 s/n 439
ARM: EC67, DIAG: EC87, REL: EC85

45m 10mm POLYESTER
10m ½" CHAIN

WATER DEPTH 4814m

850kg ANCHOR


MOORED DATA BUOY

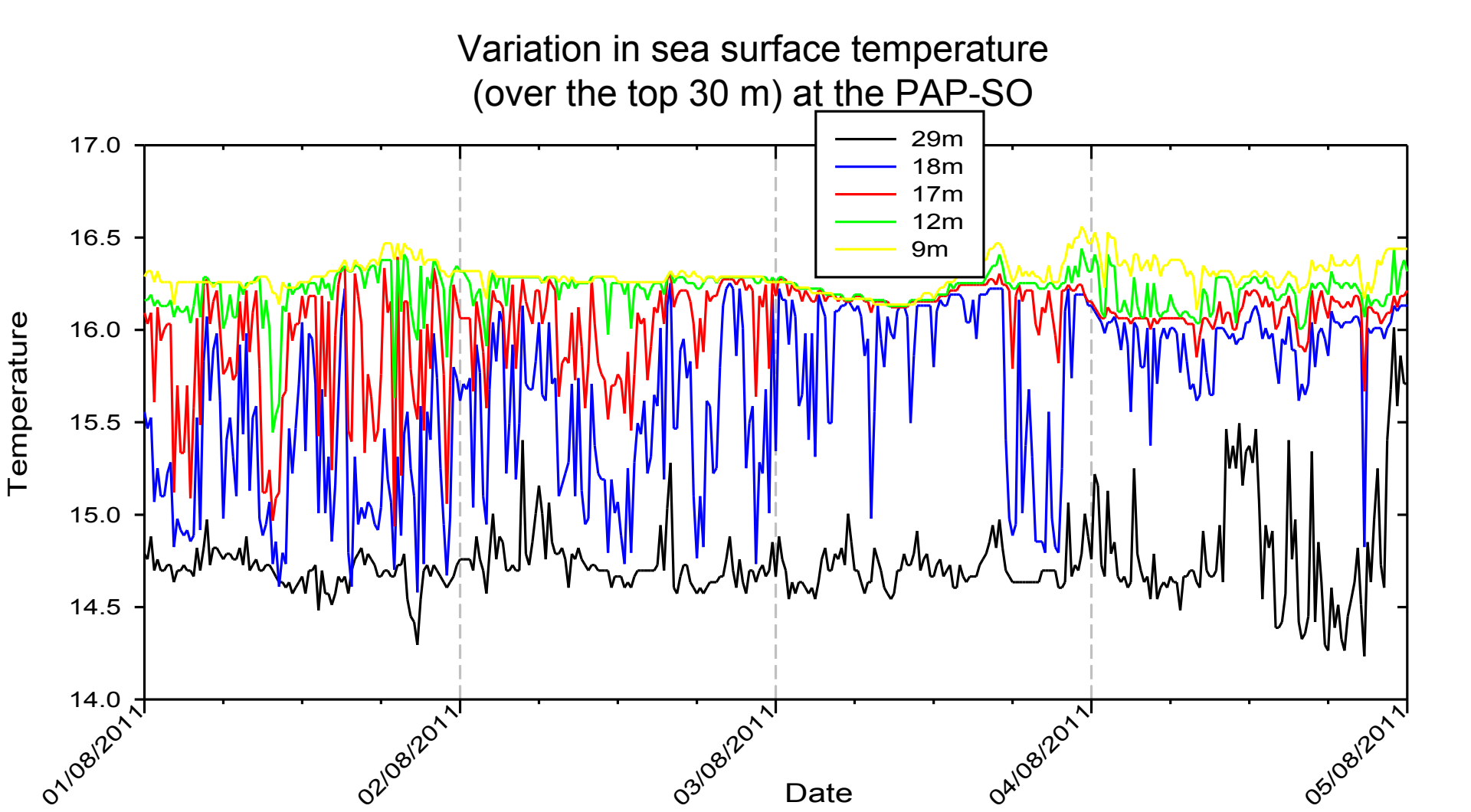
Variation in sea surface temperature
(over the top 30 m) at the PAP-SO
29m
18m
17m
12m
9m
17.0
16.5
16.0
15.5
15.0
14.5
14.0
Temperature
01/08/2011
02/08/2011
03/08/2011
04/08/2011
05/08/2011
Date

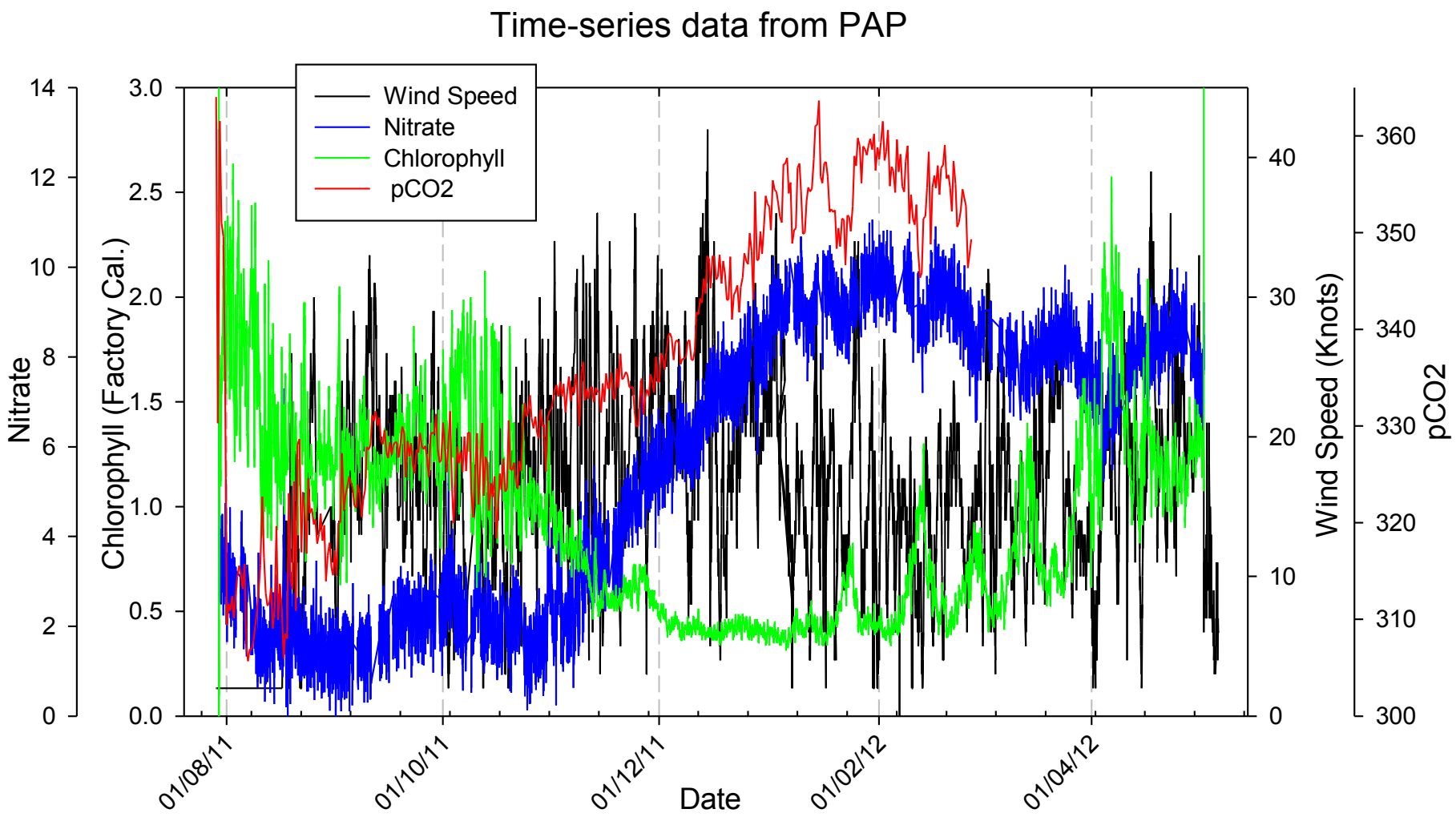

Aug. 2011 – May 2012

Data from 30 m depth from recent deployment of the PAP-SO:

Nitrate & pCO_2 increases with convective mixing in the winter months as chlorophyll-fluorescence decreases.

PAP-SO Air/sea CO_2 flux 2010, calculated using Nightingale parameterization

Illustrates that PAP is a CO_2 'sink'

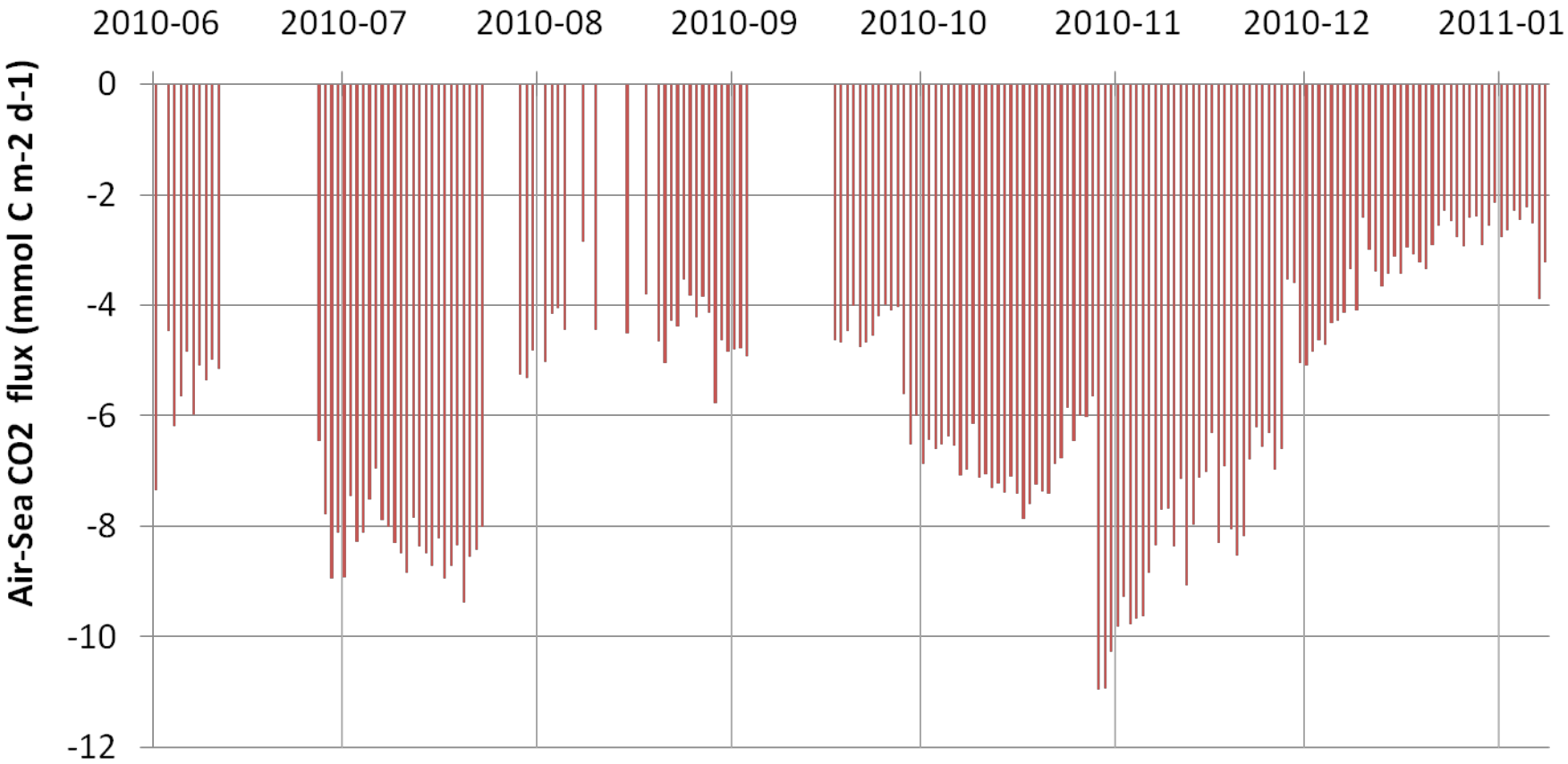

Variability at the PAP site

Decrease in nitrate

Not due to winter mixing

Hartman et al., 2010

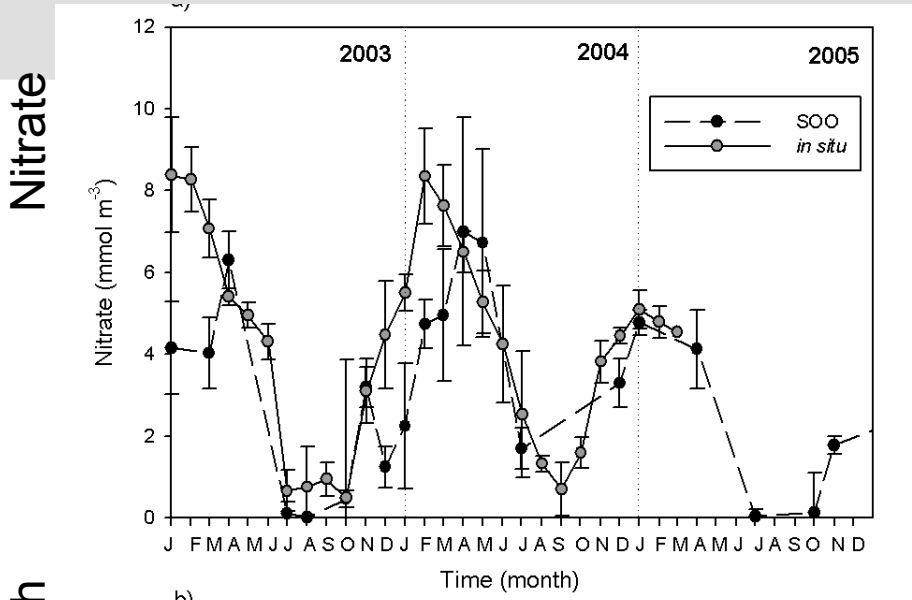

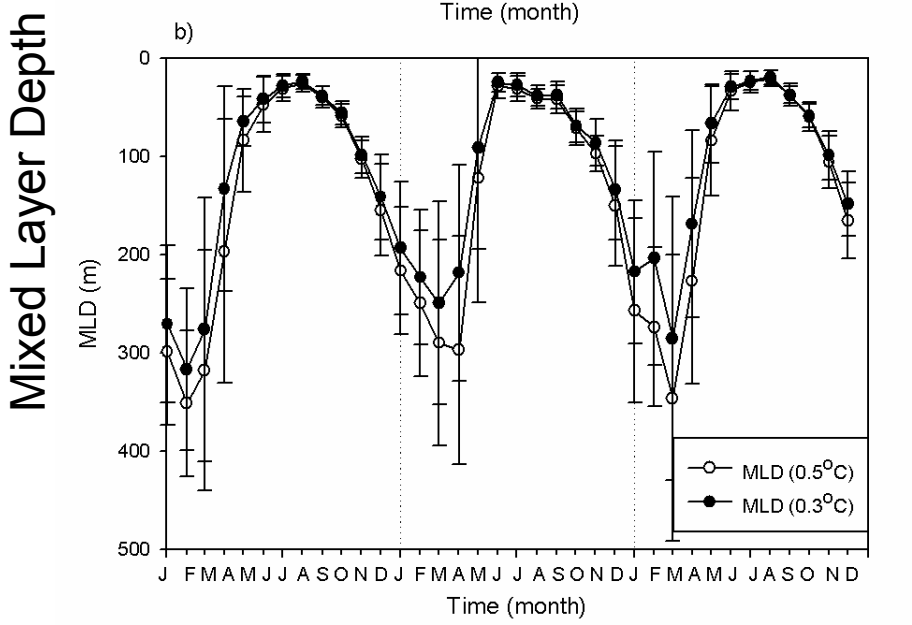

Progressive changes 2003-2005 Variability in source waters

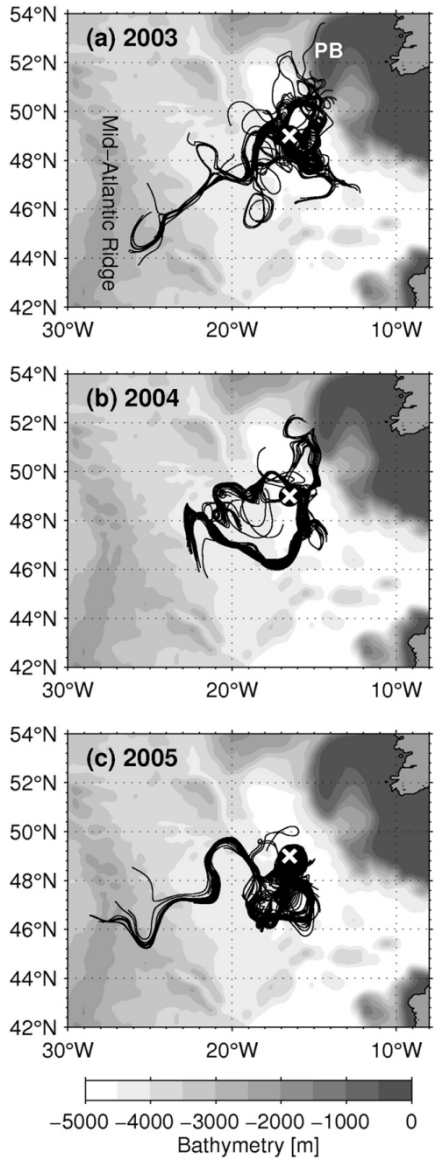

Hartman et al., 2010

Mixed Layer Depth

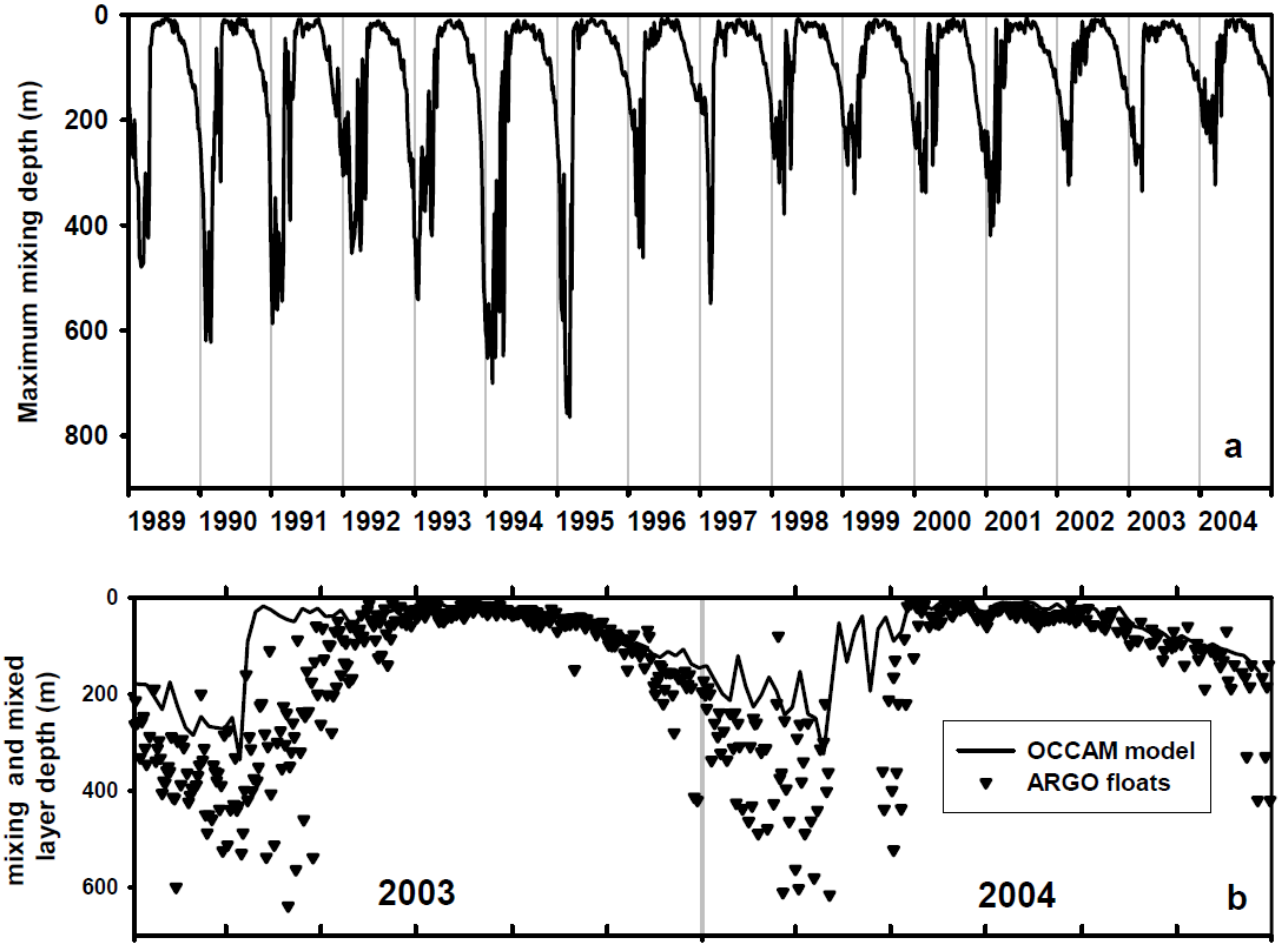

Maximum mixing depth derived from the ¼ degree OCCAM model in a circle around the PAP site with radius of 200km.(b)Expansion of data in part a(above) with the addition of plus data derived from ARGO floats which became sufficiently abundant after 2002.

Lampitt et al. 2010

Time-series analysis in Marine science and applications for industry

Mixed Layer Depth

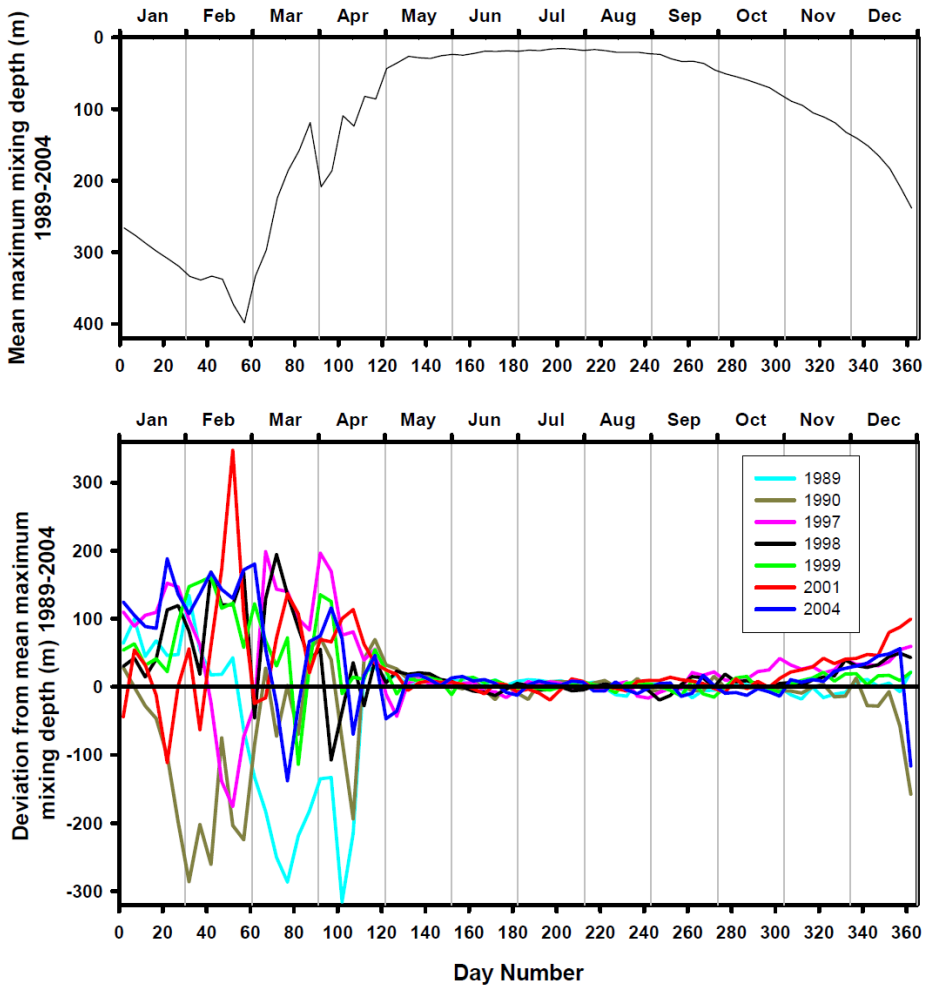

Mean maximum mixing depth determined from the 200km radius area around PAP by the ¼ degree OCCAM model. Lower: Deviation from the mean mixing depth for each of the 7 years for which there are adequate particle flux data.

Time-series analysis in Marine science and applications for industry

Chl-a

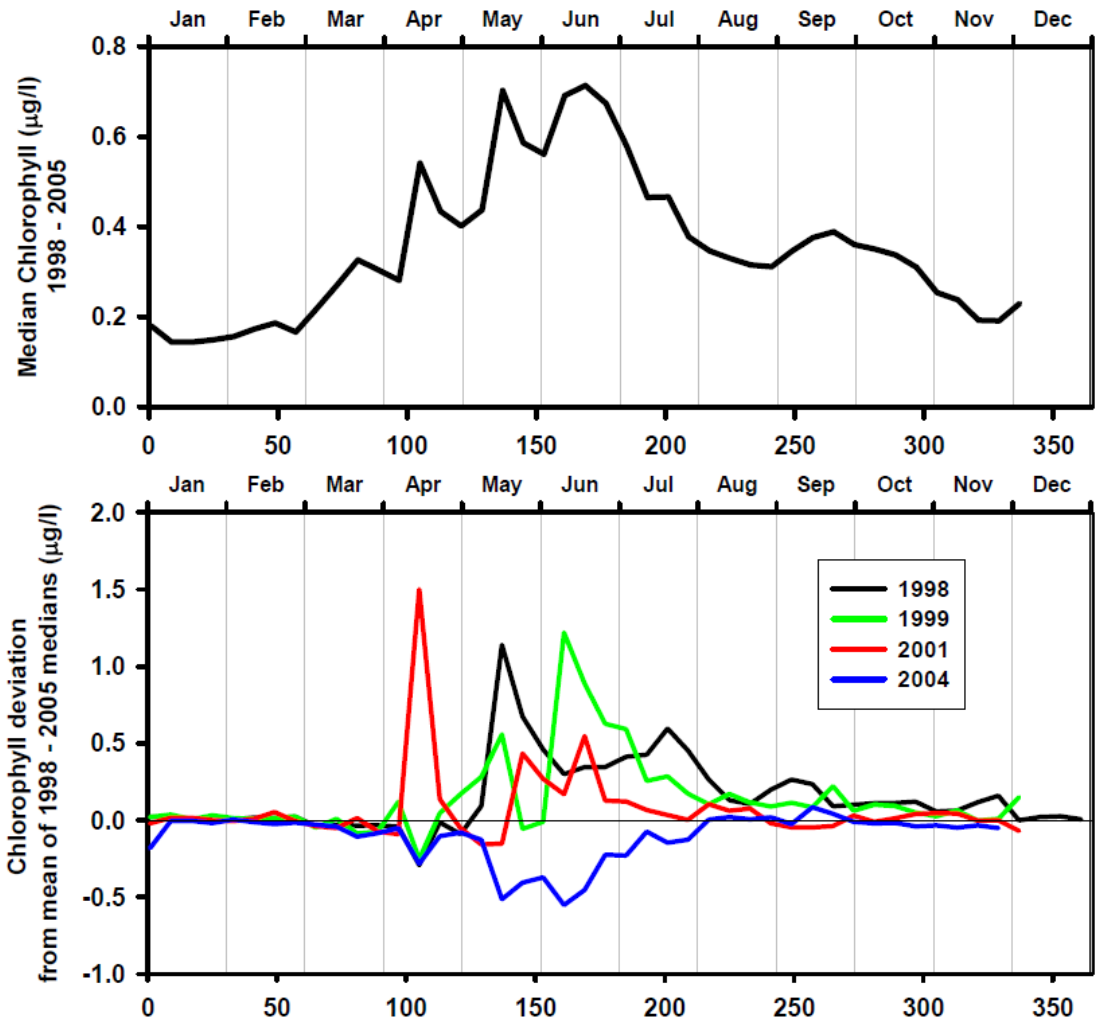

Logonna-Daoulas (France)

17-22 sept. 2012

PAP 3
Deployed JC062
27/7/2011
48°59.382' N
16°29.585' W

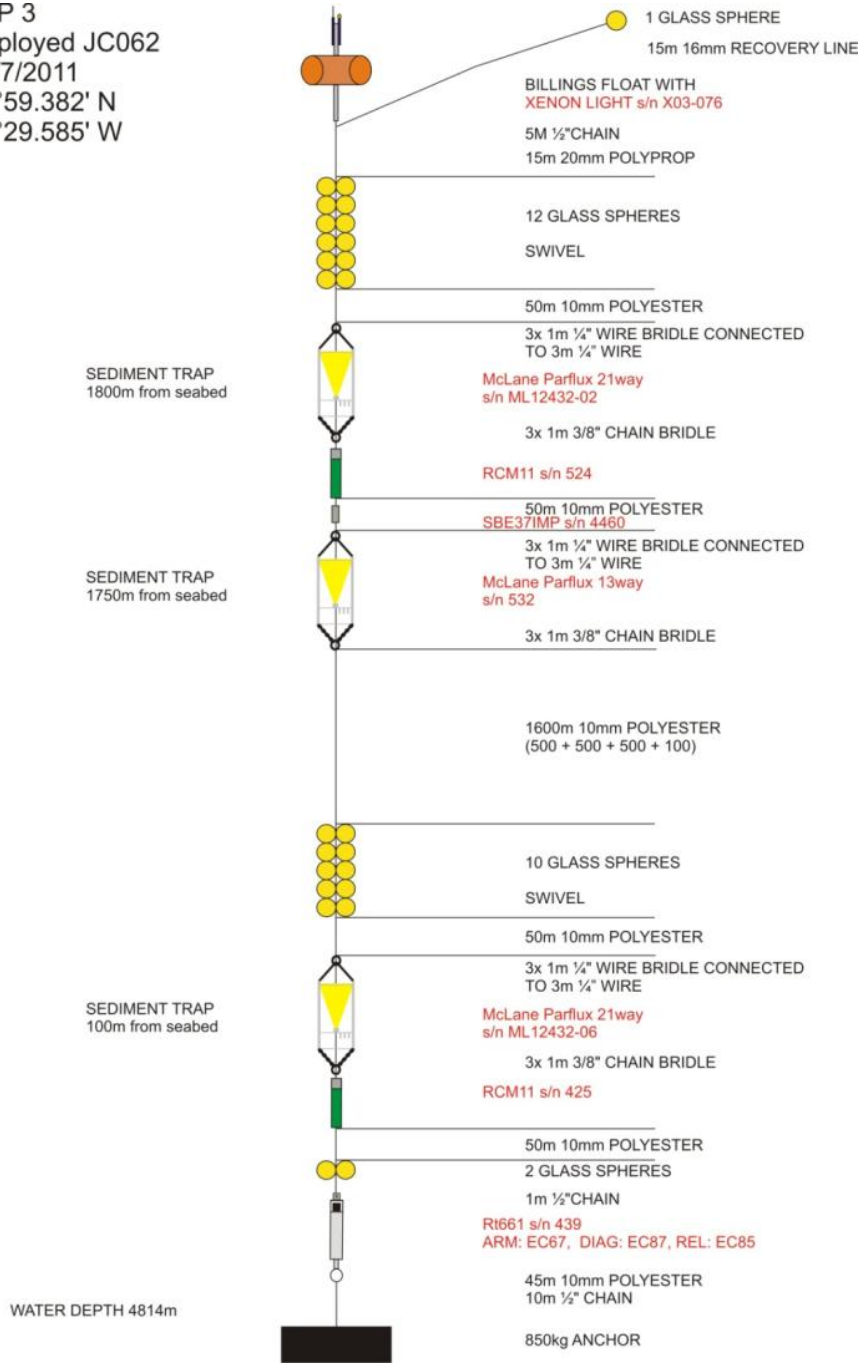

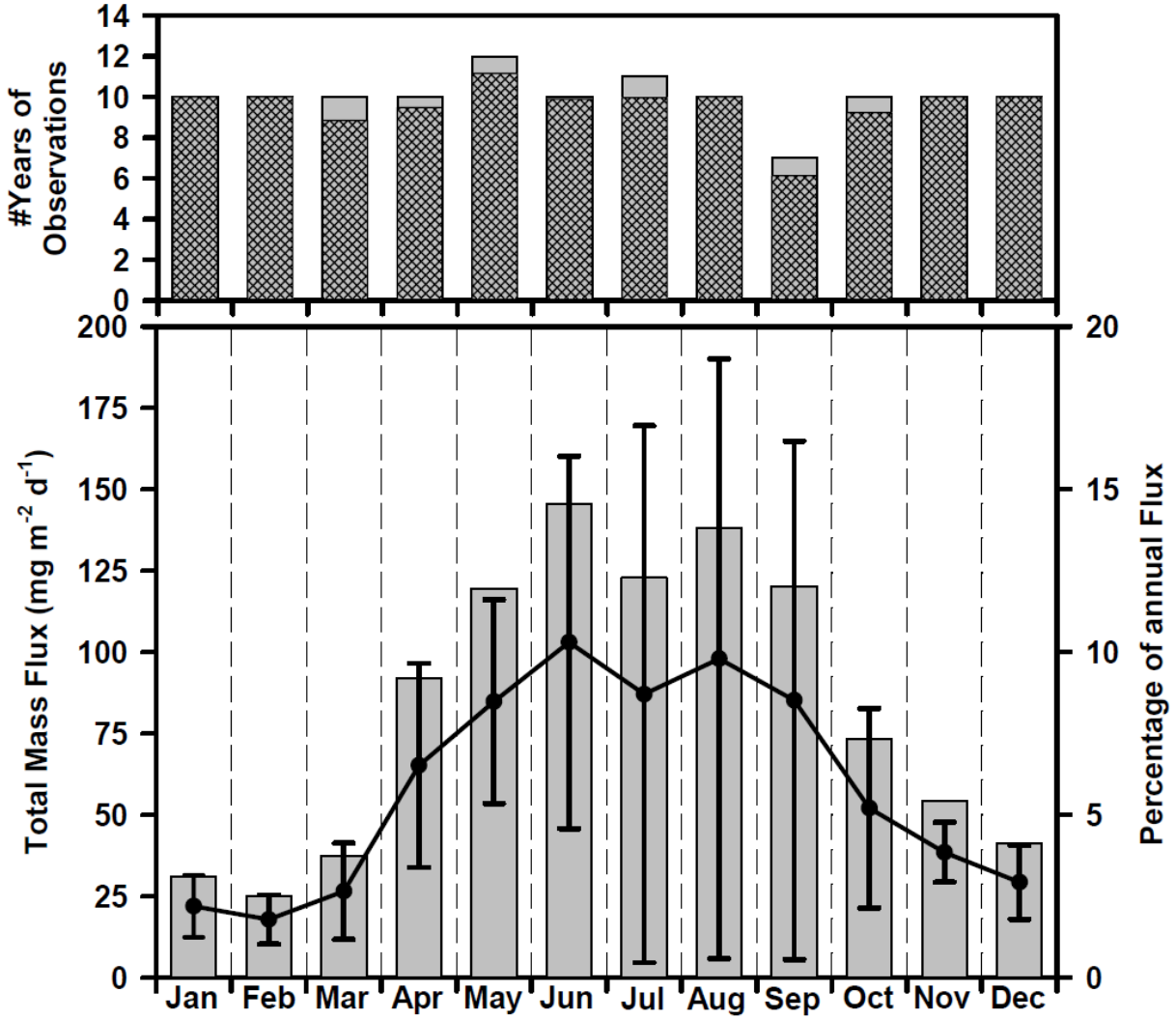

Seasonal cycle of mass flux at 3000 m based on averages of all measurements made between 1989 and 2005. In top panel bars represent the number of years for which there is greater than 15 days of flux data per month. The hatched area is the coverage co-efficient. In the bottom panel grey bars represent the percentage of annual flux each month contributes. Line plot is the average total mass flux for each individual month with error bars representing ± 1 standard deviation.

What are the levels and long term trends in particle flux?

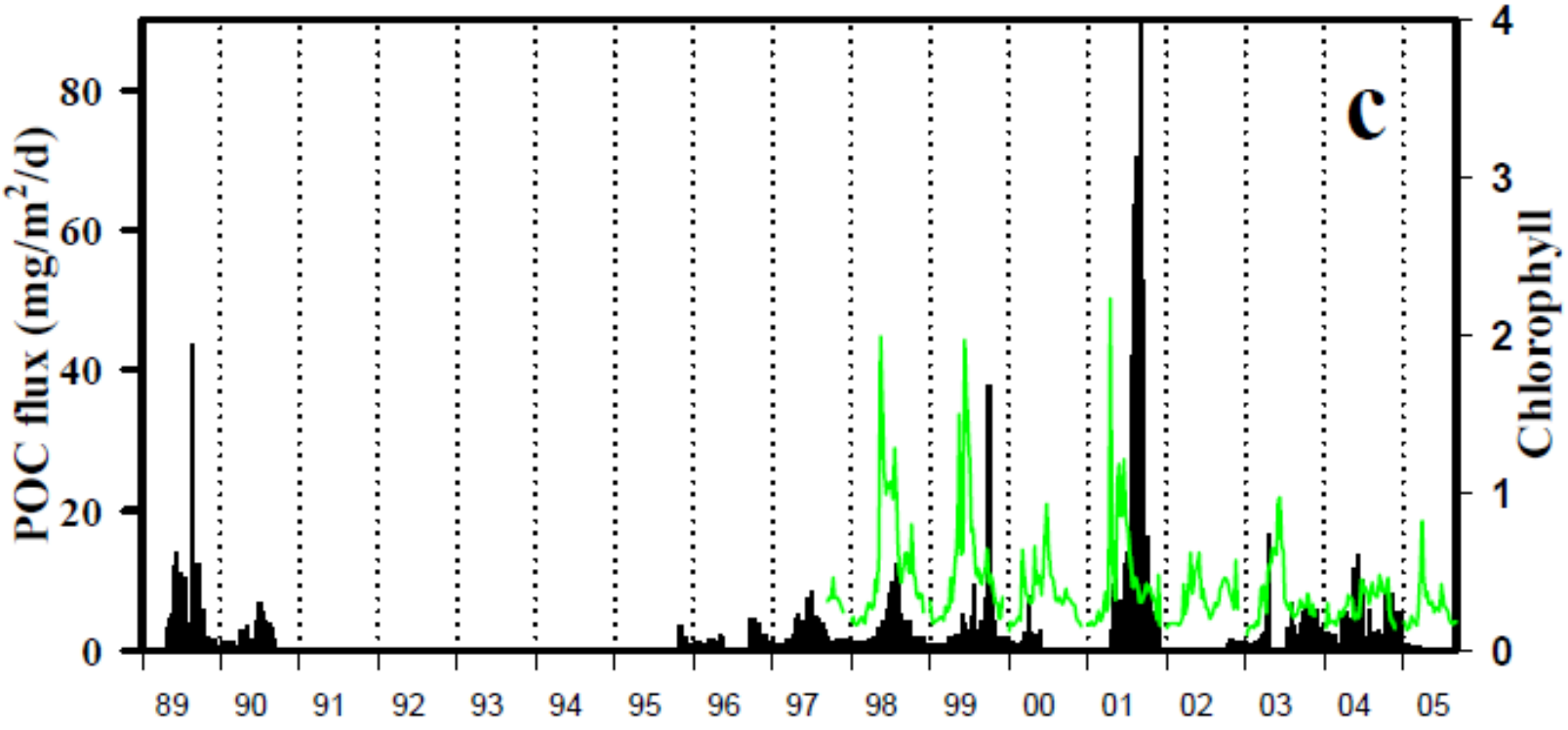

Particulate downward flux at 3000 m depth in terms of
(A)dry weight, (B) biogenic silica, (C) organic carbon and (D) inorganic carbon.
(B)Also shown (green) are the surface chlorophyll concentrations averaged over a circle of 200 km radius around the PAP site.

Lampitt et al. 2010

Phenology

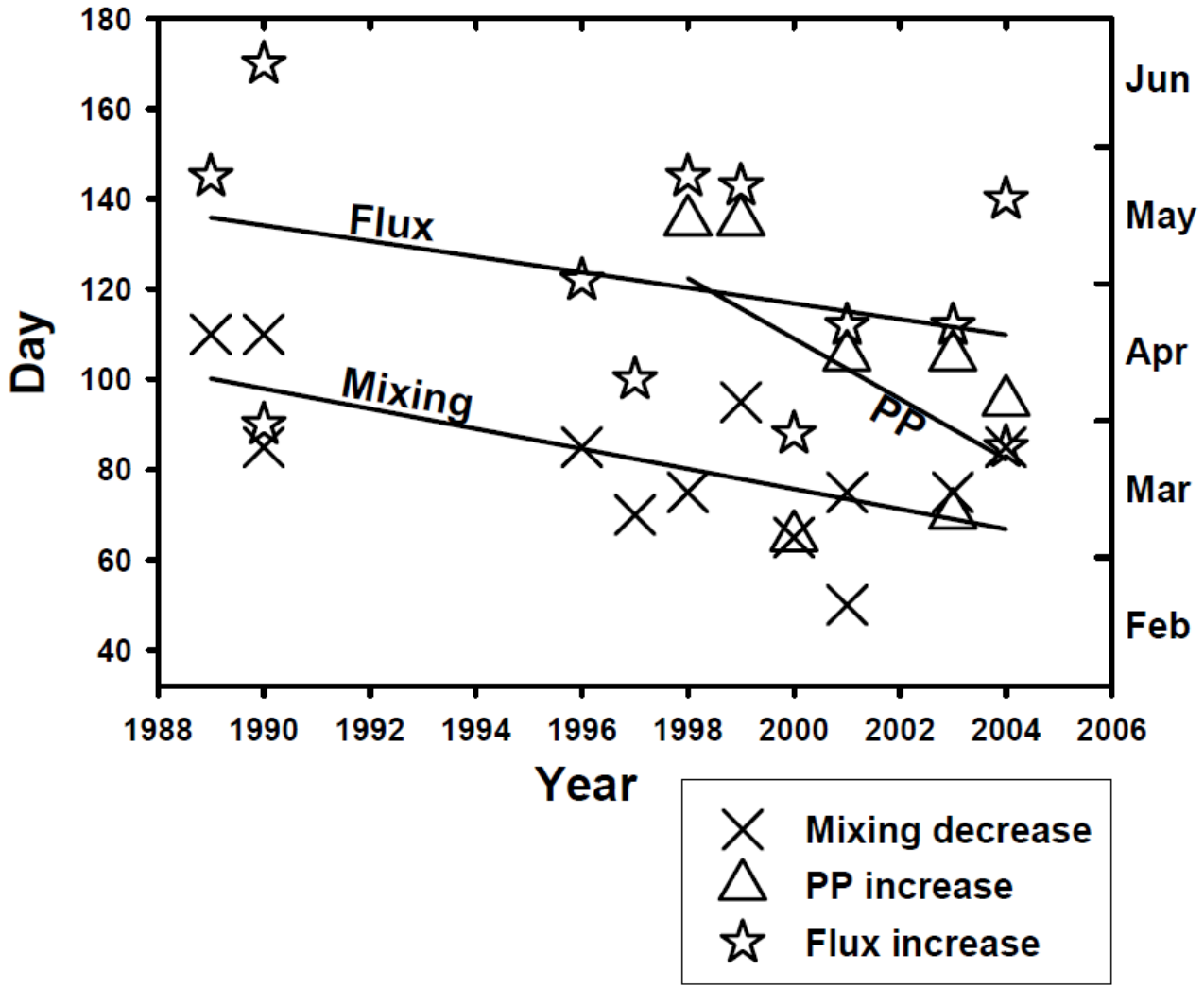

Are spring-time changes at the PAP site as reflected in the time at which mixing decreases, productivity increases and deep ocean flux increases?

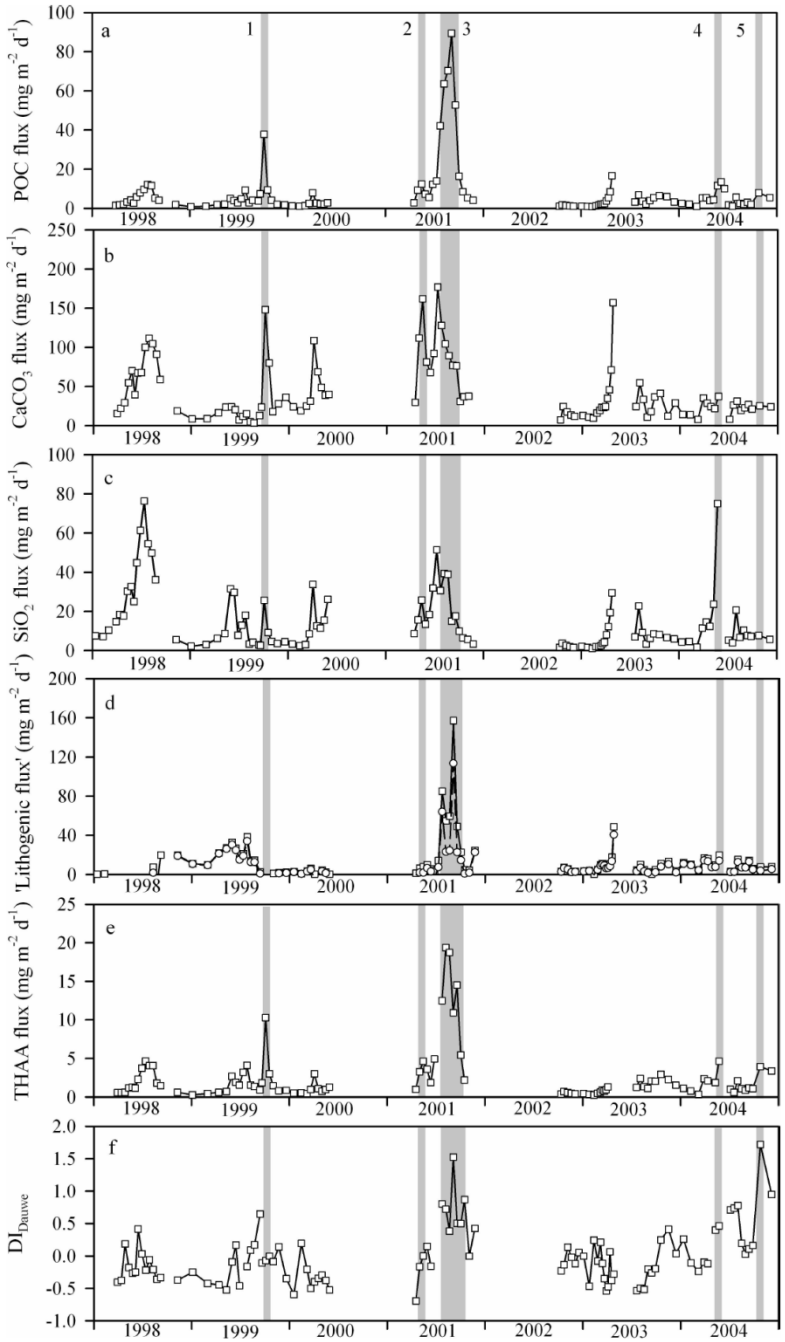

Fig. 2. Interannual variability in the fluxes of (a) POC, (b) $CaCO_3$, (c) SiO_2, (d) lithogenic matter, (e) total hydrolysable amino acids (THAA), and (f) calculated degradation index. The lithogenic flux (a) has been calculated according to Eq. 1 using POC to POM scaling factors (S) of

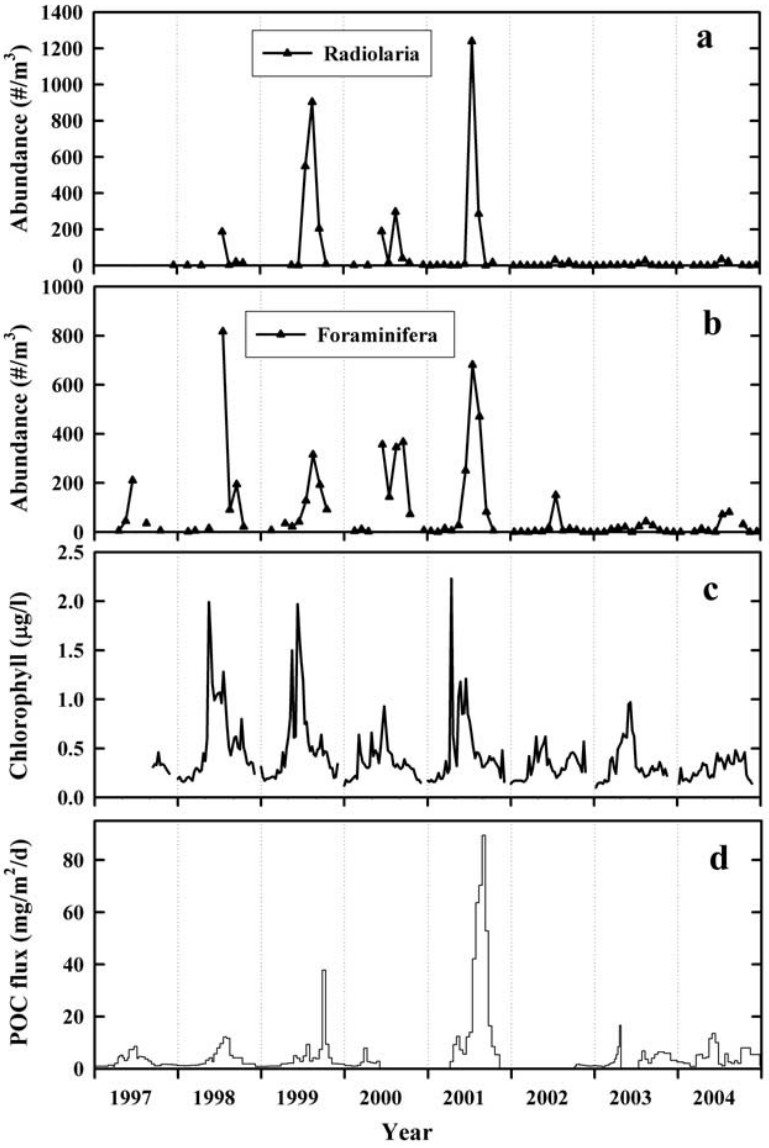

Temporal variation in (a) abundance of radiolarian and (b) abundance of foraminifera, (c) mean chlorophyll concentration around the PAP site, and (d) POC flux at 3000 m.

Faecal Pellet Fluxes

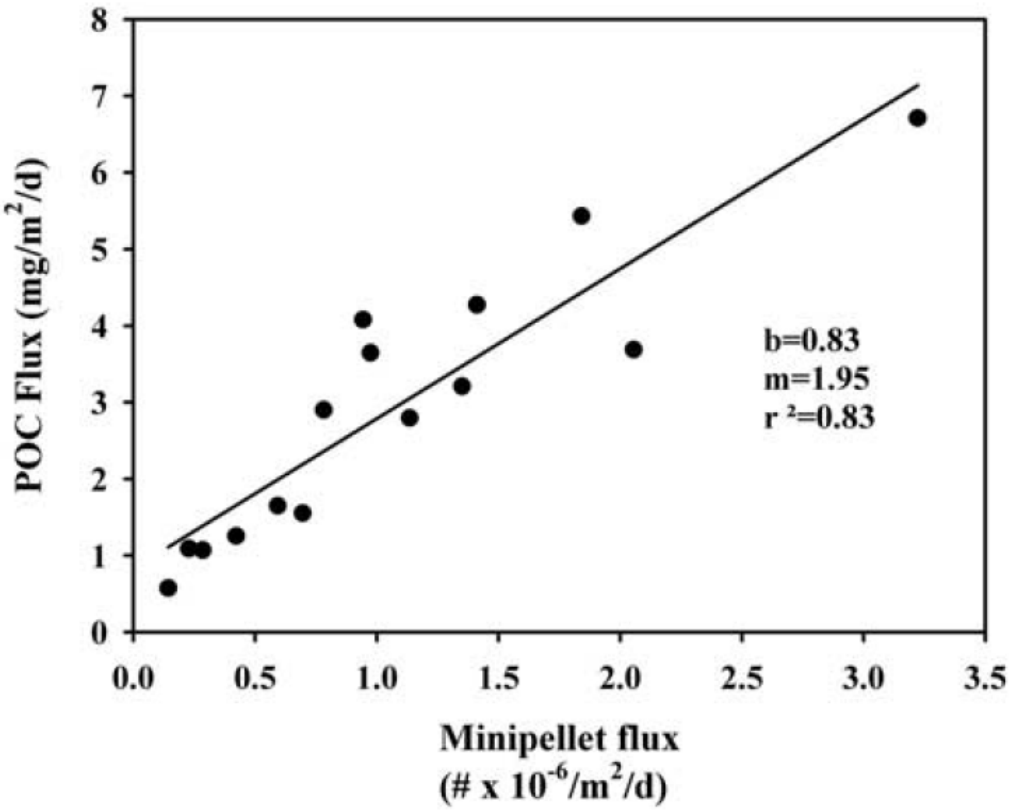

Figure 6. Relationship between downward flux of mini-pellets and POC during 1990 at 3000 m depth.

Time-series

2012

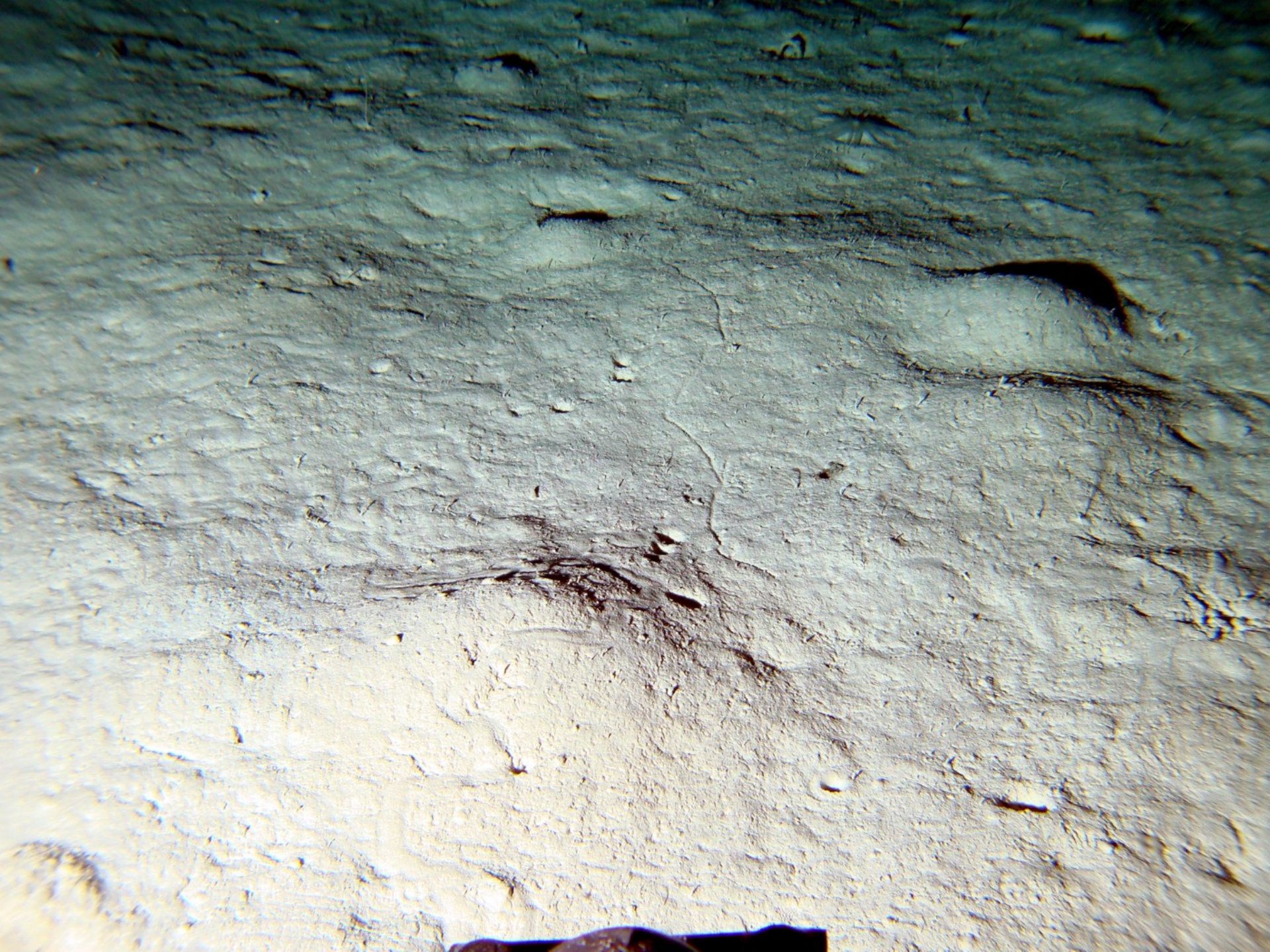

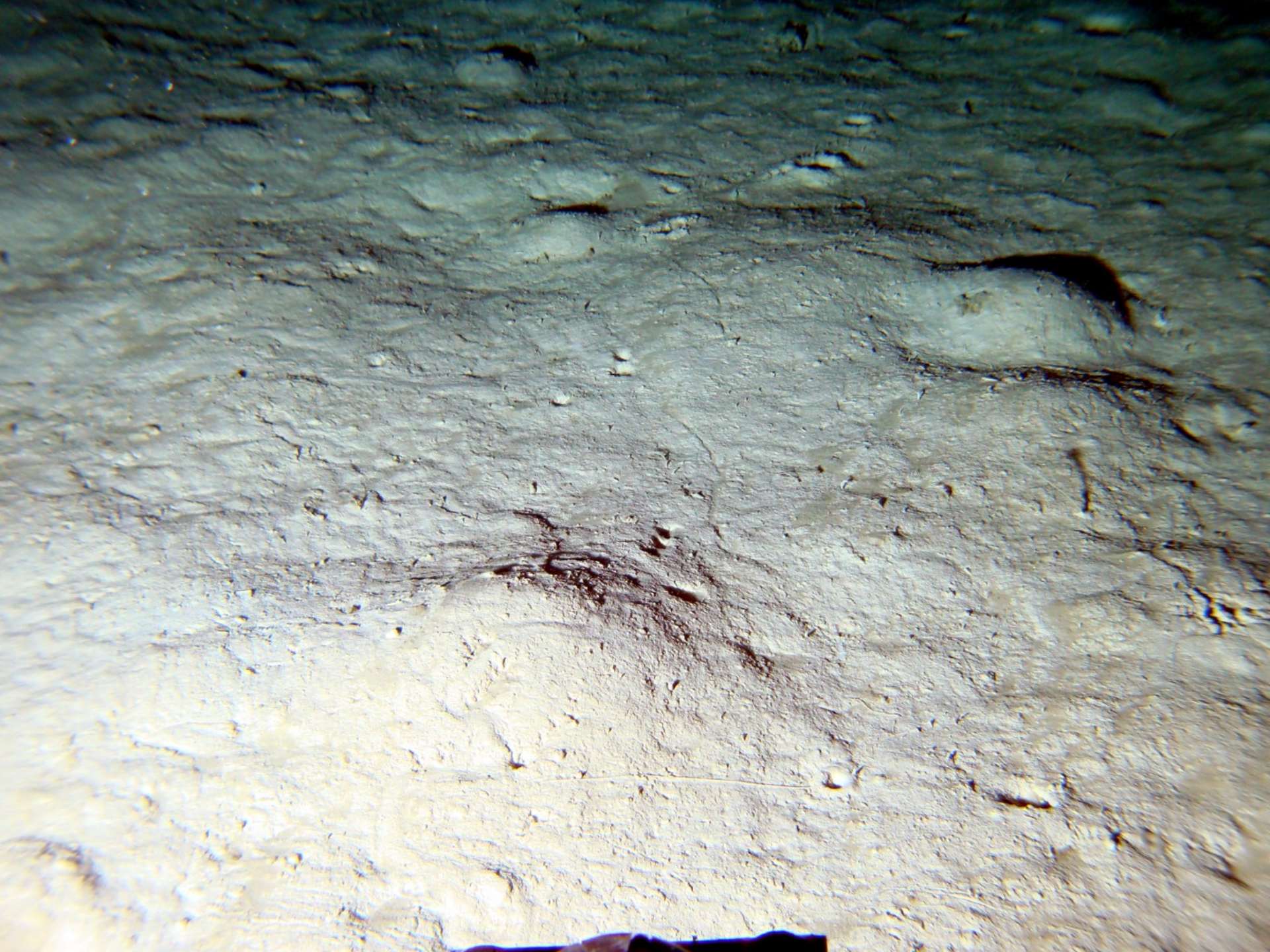

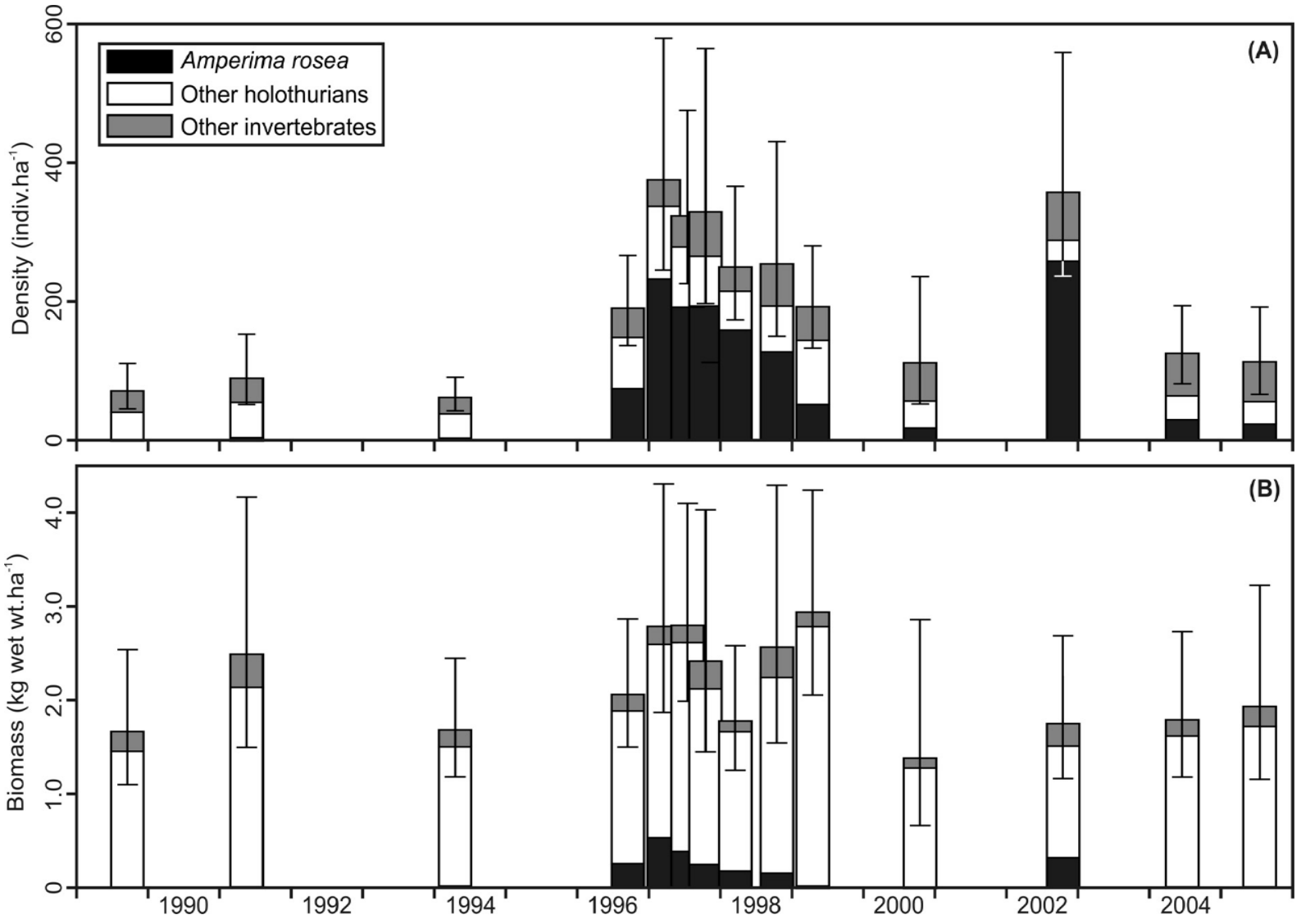

(A) density and (B) biomass of 8 selected megafaunal groups at the Porcupine Abyssal Plain Sustained Observatory site 9 (means and 95% confidence intervals are shown).

Size Distribution Variation

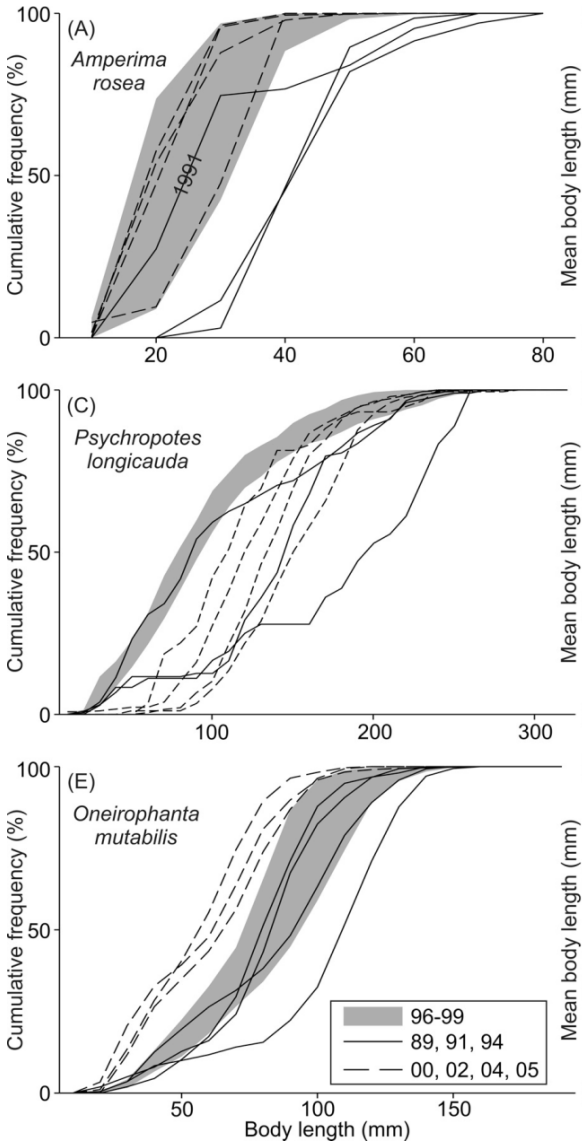

Cumulative frequency distributions of body length;

Size Distribution Variation & Respiration

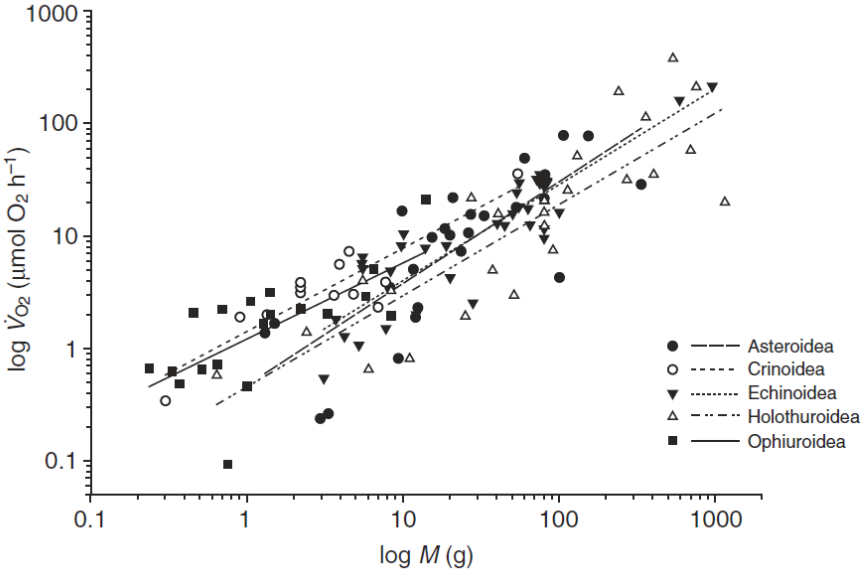

Fig. 2. Metabolic rates ($\dot{V}_{O_2}$) of the five echinoderm classes as a function of wet mass (M) as collated in the final echinoderm metabolic rate data set (see text). Scaling relationships are in the form $\dot{V}_{O_2}=aM^b$ where a is a normalisation constant and b is a scaling coefficient representing the slope of the relationship between $\dot{V}_{O_2}$ and M. The metabolic rates of all five echinoderm classes are highly significantly correlated with mass ($P<0.001$): Asteroidea ($0.472M^{0.90}$, $R^2=0.636$), Crinoidea ($1.414M^{0.74}$, $R^2=0.792$), Echinoidea ($0.564M^{0.85}$, $R^2=0.796$), Holothuroidea ($0.456M^{0.81}$, $R^2=0.730$), Ophiuroidea ($1.215M^{0.68}$, $R^2=0.481$). All metabolic rates have been normalised to 12°C using a Q_{10} adjustment of 2.15. Sources of all data can be found in supplementary material Table S1.

We then took our avg. body size data for each taxon and converted that to individual respiration rates.

We then multiplied the individual respiration rates by animal density for all the dominant taxa to get community respiration rates.

Which then gave us...

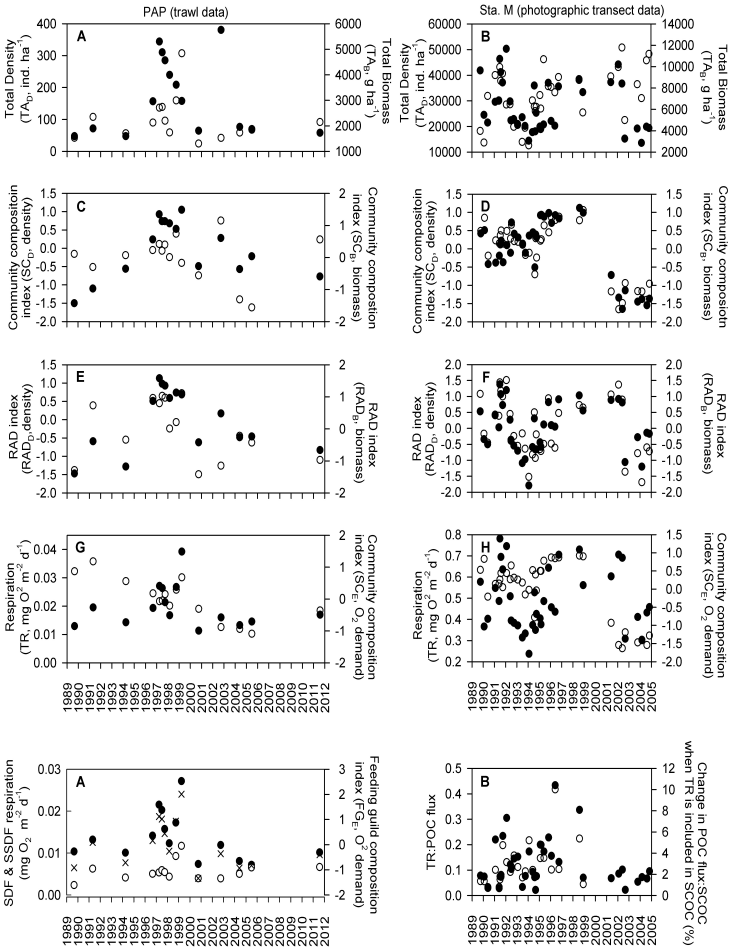

Time series of echinoderm megafauna community dynamics for the PAP and Sta. M research sites including A and B) density (●, TA_D), biomass (◦, TA_B); C and D) indices of species composition similarity based on density data (●, SC_D) and biomass (◦, SC_B); E and F) indices of rank abundance distribution similarity based on density (●, RAD_D) and biomass (◦, RAD_B); and G and H) total respiration of the studied megafauna (●, TR) and an index of species composition similarity based on energetic demand (◦, SC_E).

Ruhl et al., in prep

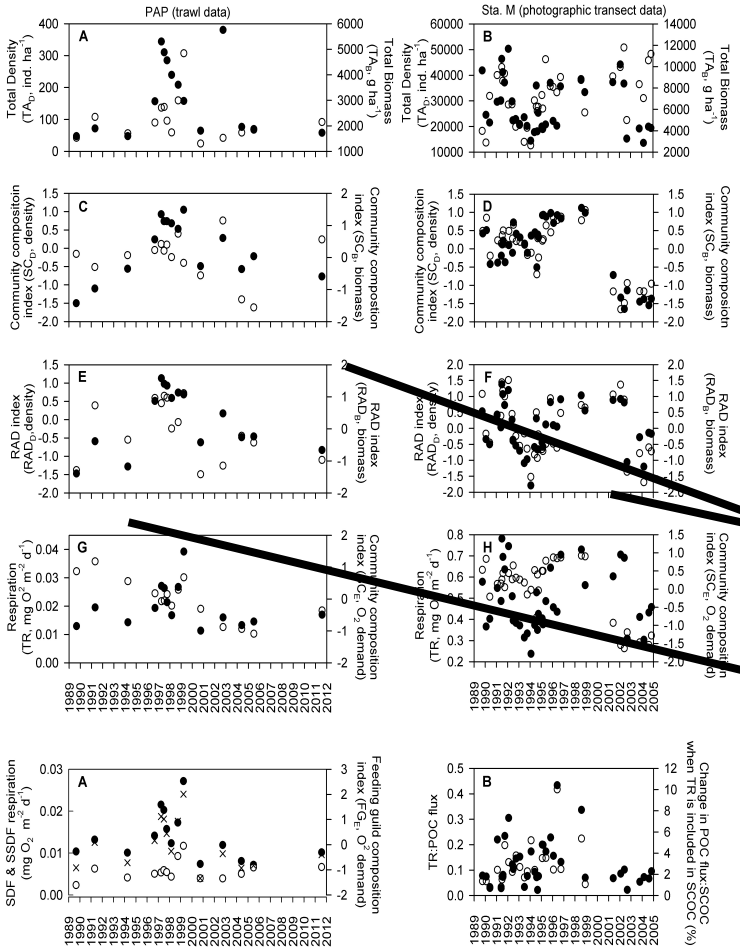

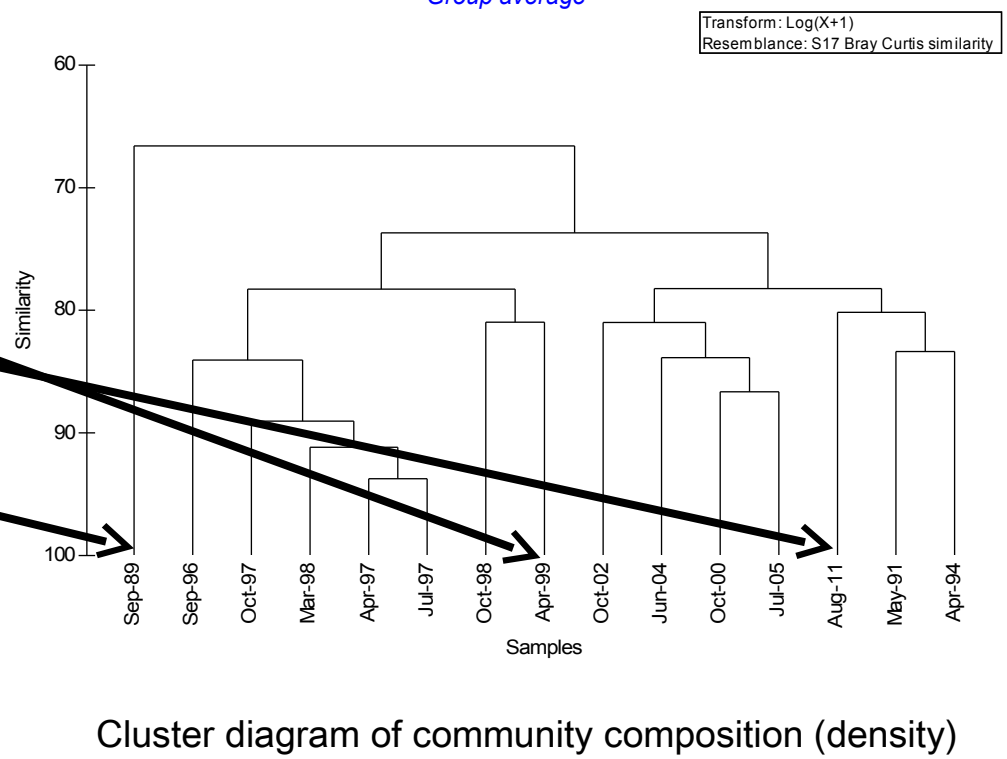

Cluster diagram of community composition (density)

Time series of echinoderm megafauna community dynamics for the PAP including A) density (●, TA_D), biomass (◦, TA_B); C) indices of species composition similarity based on density data (●, SC_D) and biomass (◦, SC_B); E) indices of rank abundance distribution similarity based on density (●, RAD_D) and biomass (◦, RAD_B); and G) total respiration of the studied megafauna (●, TR) and an index of species composition similarity based on energetic demand (◦, SC_E).

Ruhl et al., in prep

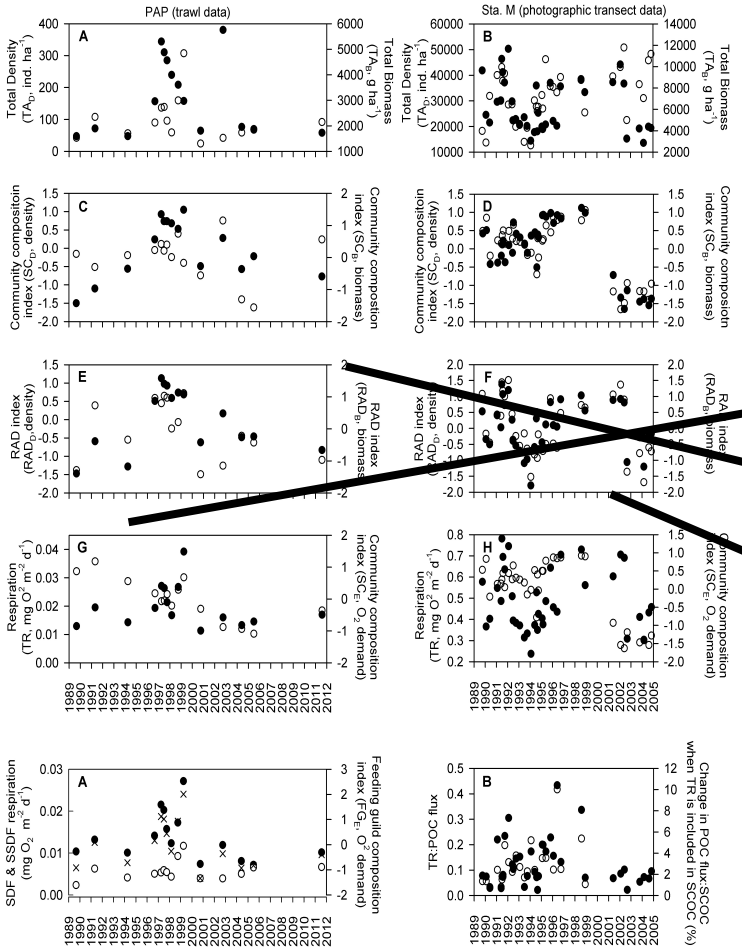

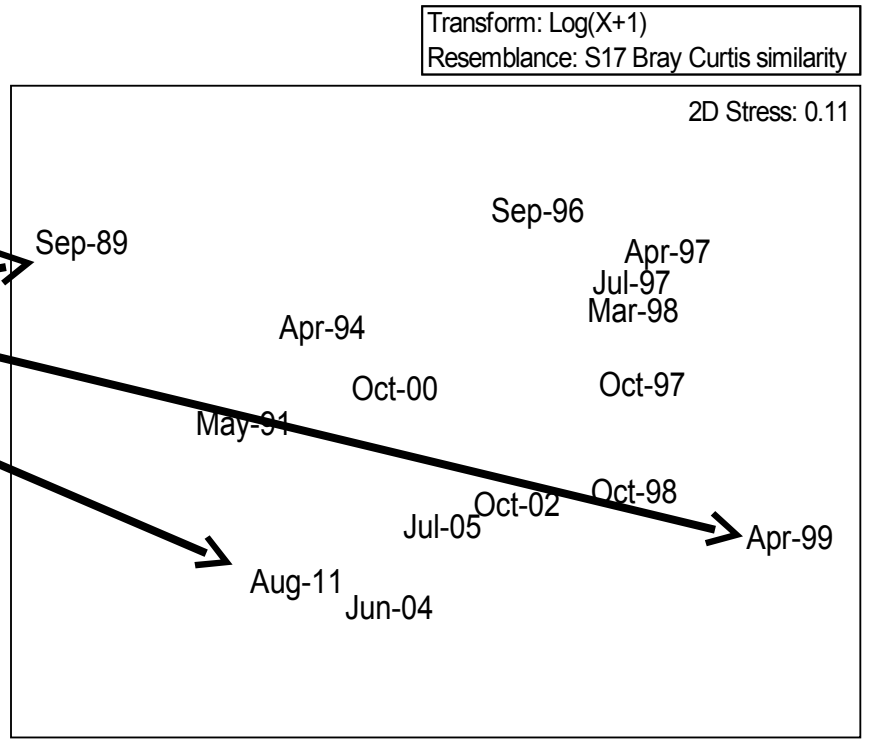

MDS plot of community composition (density), x-axis used as y axis for time series

Time series of echinoderm megafauna community dynamics for the PAP and Sta. M research sites including A and B) density (●, TA_D), biomass (◦, TA_B); C and D) indices of species composition similarity based on density data (●, SC_D) and biomass (◦, SC_B); E and F) indices of rank abundance distribution similarity based on density (●, RAD_D) and biomass (◦, RAD_B); and G and H) total respiration of the studied megafauna (●, TR) and an index of species composition similarity based on energetic demand (◦, SC_E).

Ruhl et al., in prep

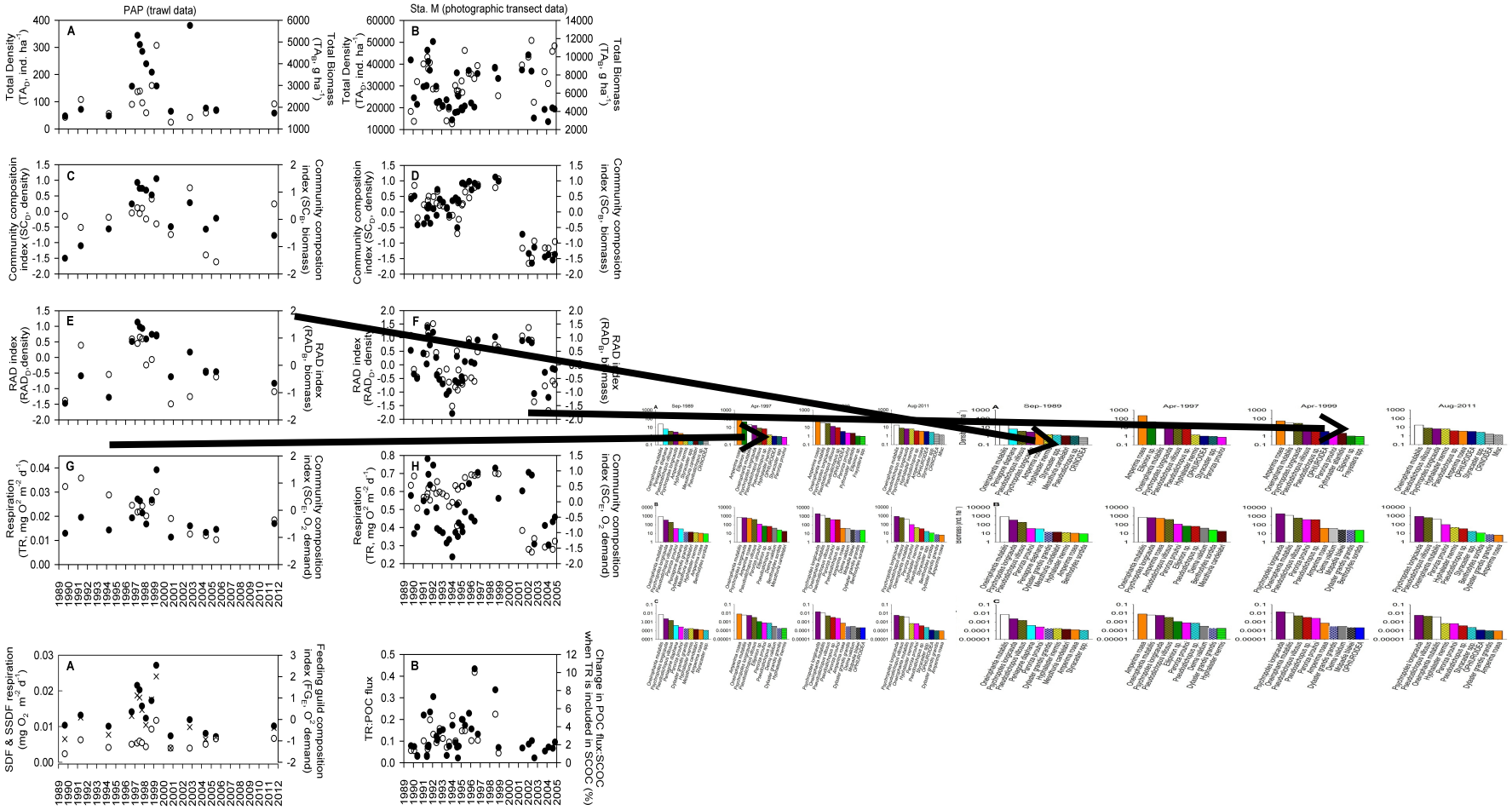

Rank abundance distribution plots

Time series of echinoderm megafauna community dynamics for the PAP and Sta. M research sites including A and B) density (●, TA_D), biomass (◦, TA_B); C and D) indices of species composition similarity based on density data (●, SC_D) and biomass (◦, SC_B); E and F) indices of rank abundance distribution similarity based on density (●, RAD_D) and biomass (◦, RAD_B); and G and H) total respiration of the studied megafauna (●, TR) and an index of species composition similarity based on energetic demand (◦, SC_E).

Ruhl et al., in prep

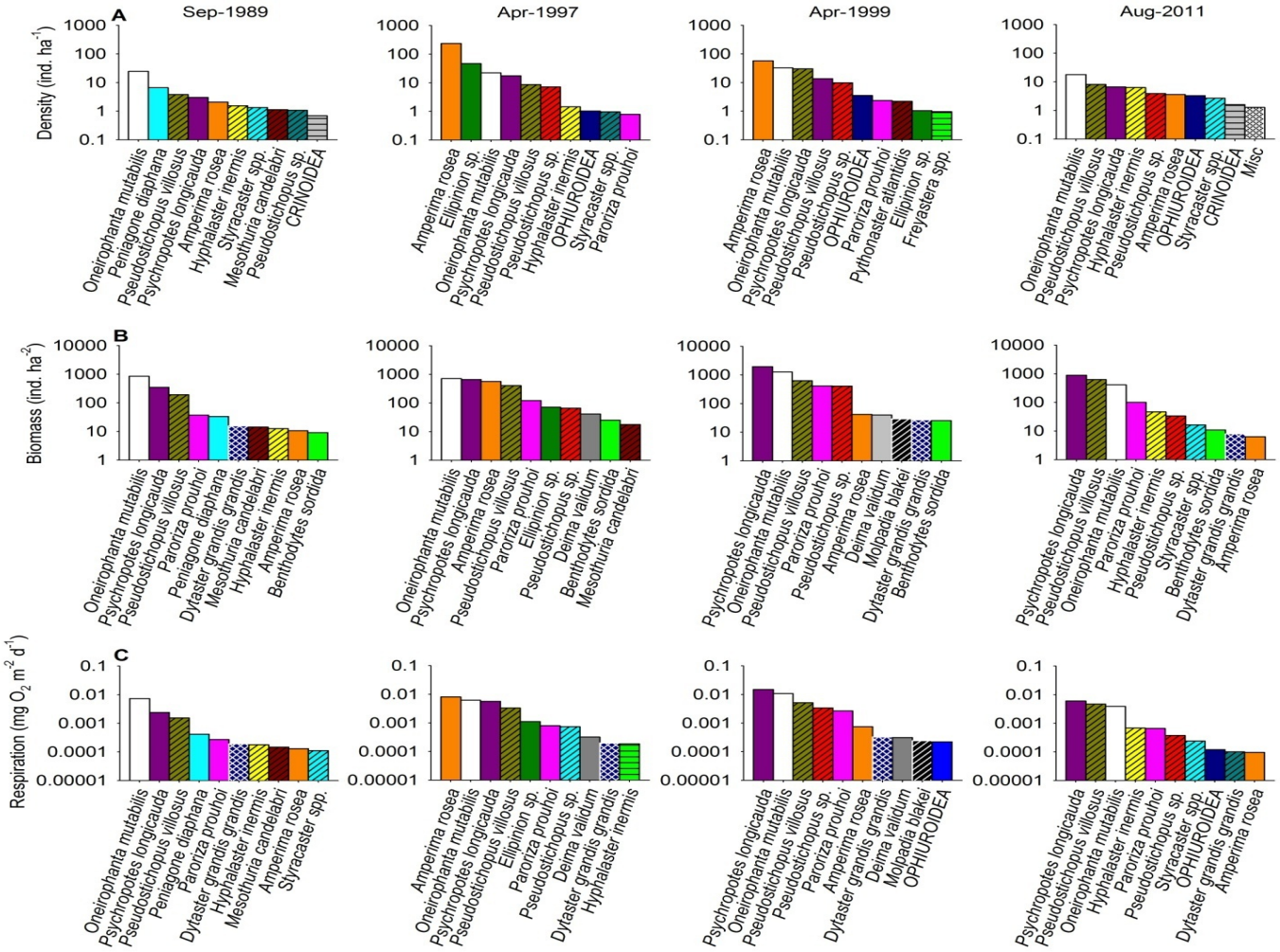

Rank abundance distribution plots for PAP data for selected times during the time series based on:

A)density;
B) biomass; and
C) energetic demand (respiration),

Illustrates both changes in distribution shape, but also the ranks of the top ten most dominant fauna over time.

The SDF are open bars, SSDF diagonally hatched bars, SF have horizontally hatched bars, and P/S are cross hatched.

Ruhl et al., in prep

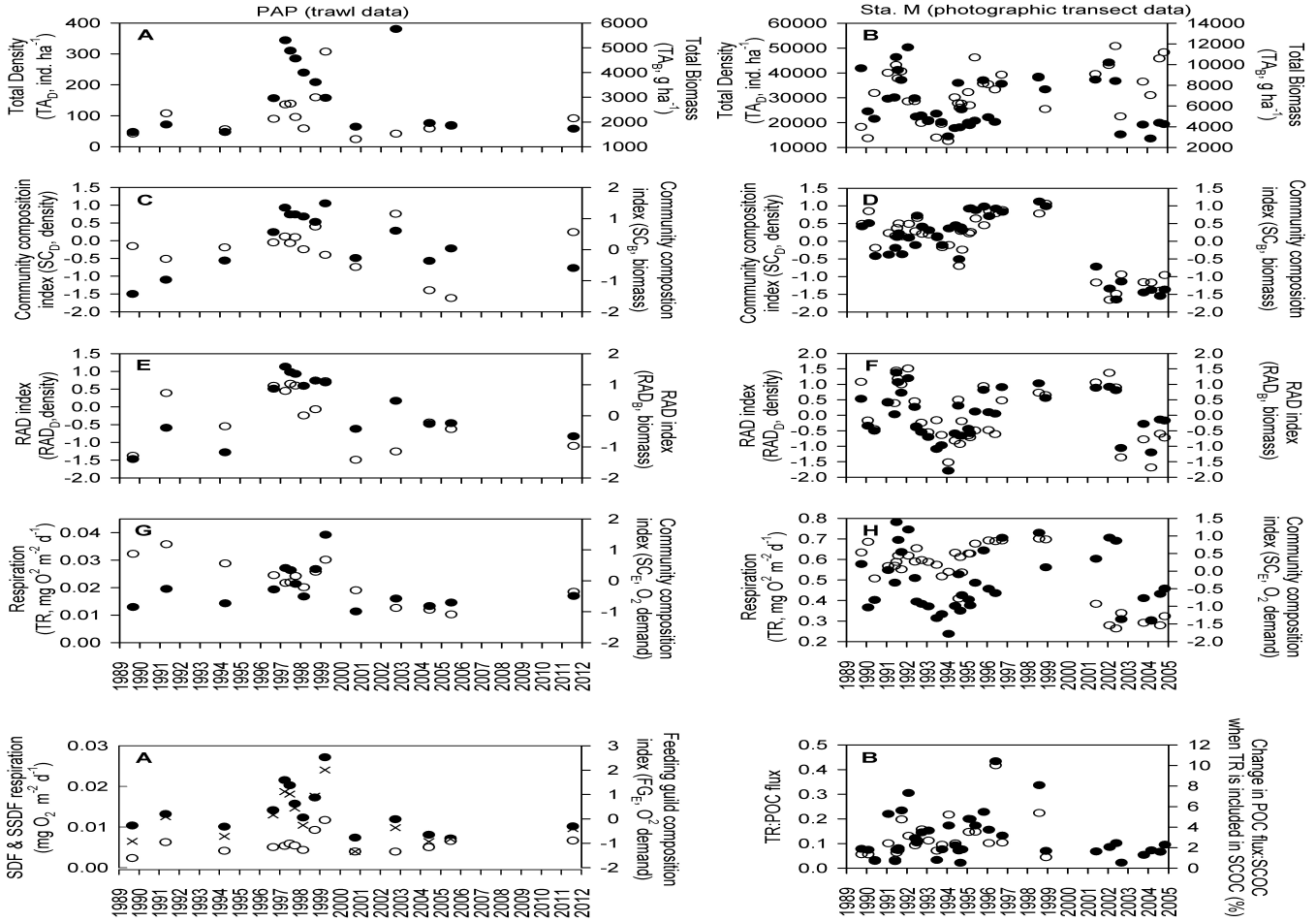

Time series of echinoderm megafauna community dynamics for the PAP and Sta. M research sites including A and B) density (●, TA_D), biomass (◦, TA_B); C and D) indices of species composition similarity based on density data (●, SC_D) and biomass (◦, SC_B); E and F) indices of rank abundance distribution similarity based on density (●, RAD_D) and biomass (◦, RAD_B); and G and H) total respiration of the studied megafauna (●, TR) and an index of species composition similarity based on energetic demand (◦, SC_E).

Ruhl et al., in prep

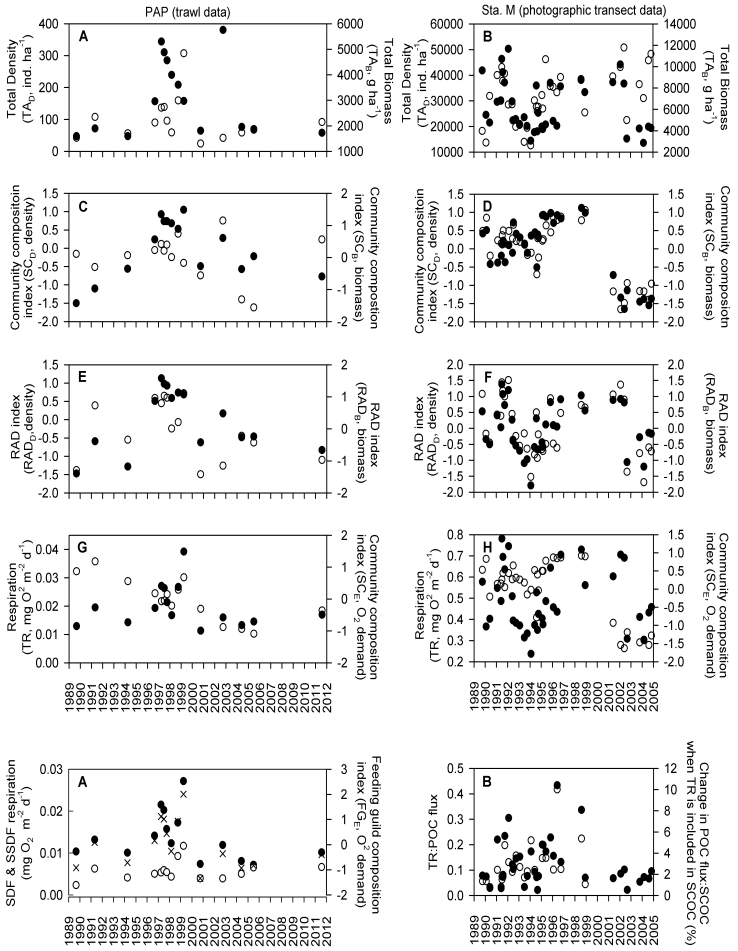

Community descriptor	Sta. M (n=37)		PAP (n=15)	
	TR	*p*	TR	*p*
univariate	r_s		r_s	
TA_D	***0.63***	***<0.001***	**0.61**	**0.02**
TA_B	***0.87***	***<0.001***	***0.94***	***<0.001***
multivariate	R	*p*	R	*p*
SC_D	**0.09**	**0.053**	**0.34**	**0.007**
SC_B	***0.31***	***<0.001***	0.20	0.07
SC_E	***0.27***	***<0.001***	**0.42**	**0.02**
RAD_D	***0.25***	***<0.001***	**0.37**	**0.004**
RAD_B	***0.70***	***<0.001***	***0.49***	***<0.001***
RAD_E	***0.75***	***<0.001***	***0.78***	***<0.001***

Time series of echinoderm megafauna community dynamics for the PAP and Sta. M research sites including A and B) density (●, TA_D), biomass (◦, TA_B); C and D) indices of species composition similarity based on density data (●, SC_D) and biomass (◦, SC_B); E and F) indices of rank abundance distribution similarity based on density (●, RAD_D) and biomass (◦, RAD_B); and G and H) total respiration of the studied megafauna (●, TR) and an index of species composition similarity based on energetic demand (◦, SC_E).

Ruhl et al., in prep

Are pigments related to change?

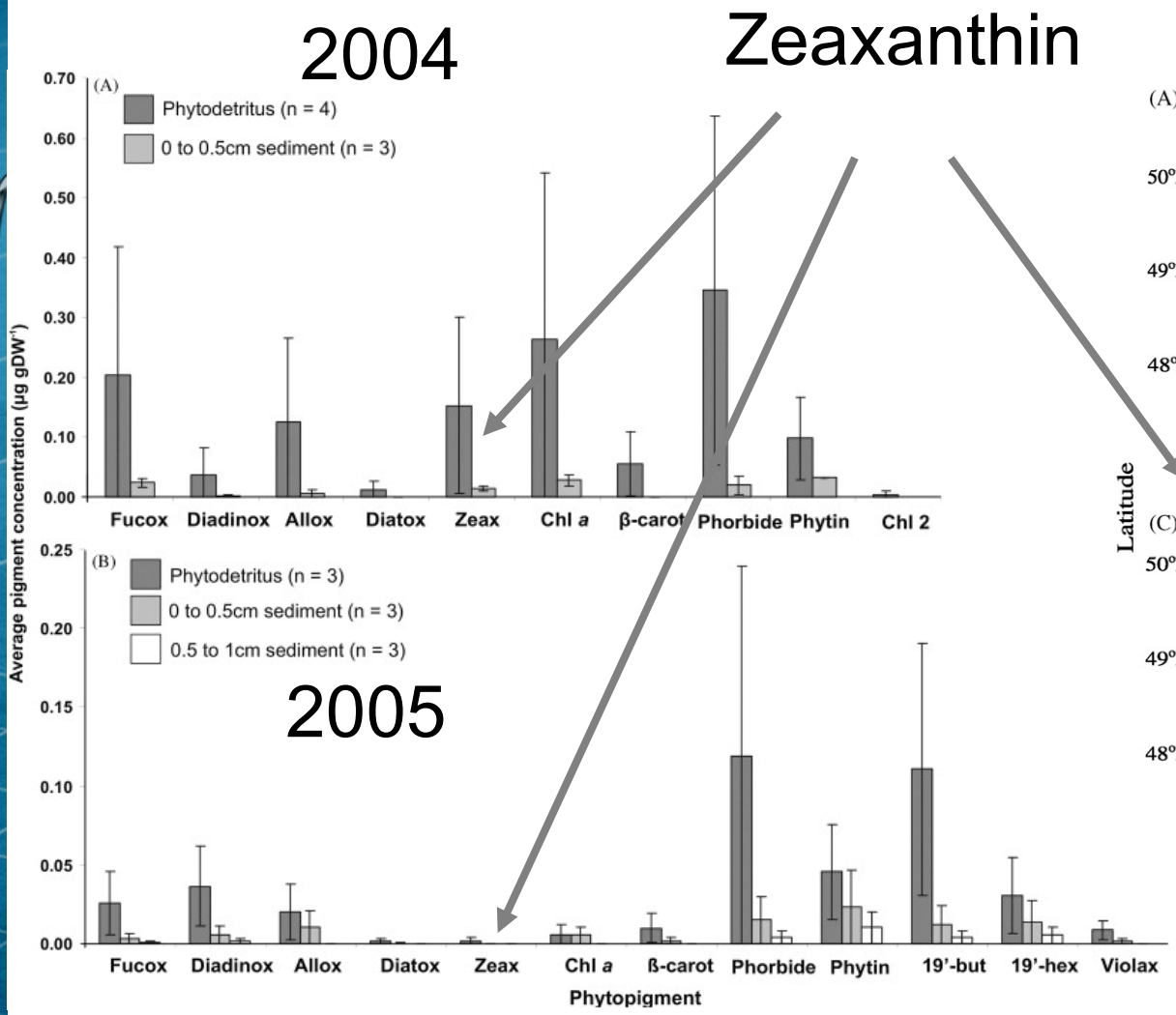

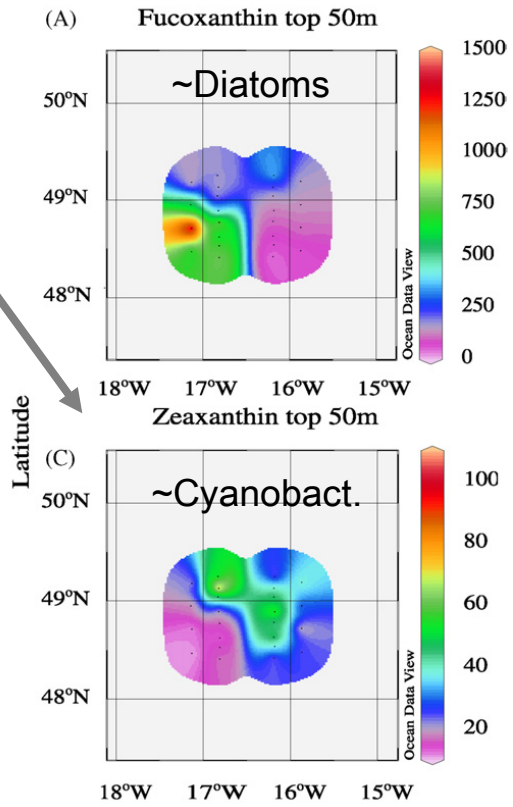

Fitz-George Balfour et al., 2010

Are pigments related to change?

MDS ordination of 37 individual holothurian ovary samples from PAP June 29 2004 (a) and July 2005 (b), based on √-transformed pigment percentage contributions 30 and Bray-Curtis similarities.

Key:
▲= *Amperima rosea*;
d = *Oneirophanta mutabilis*
■ = *Peniagone diaphana*
□ = *Psychropotes longicauda*
X = *Paroriza prouhoi*

T. Smith, Billett, Wolff, Thompson, and Tyler, Deep-Sea Res., 2010

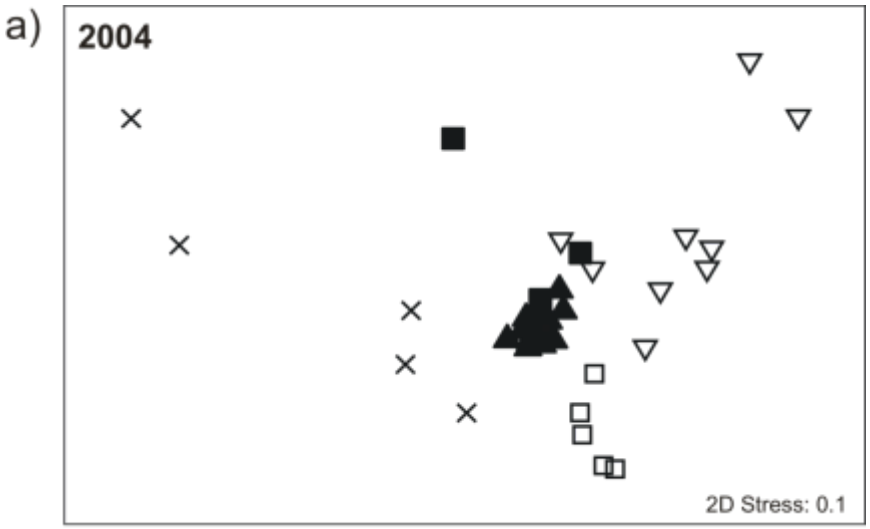

Fitz-George Balfour et al., 2010

Biogeochemical Models Suggest Major Change Ahead

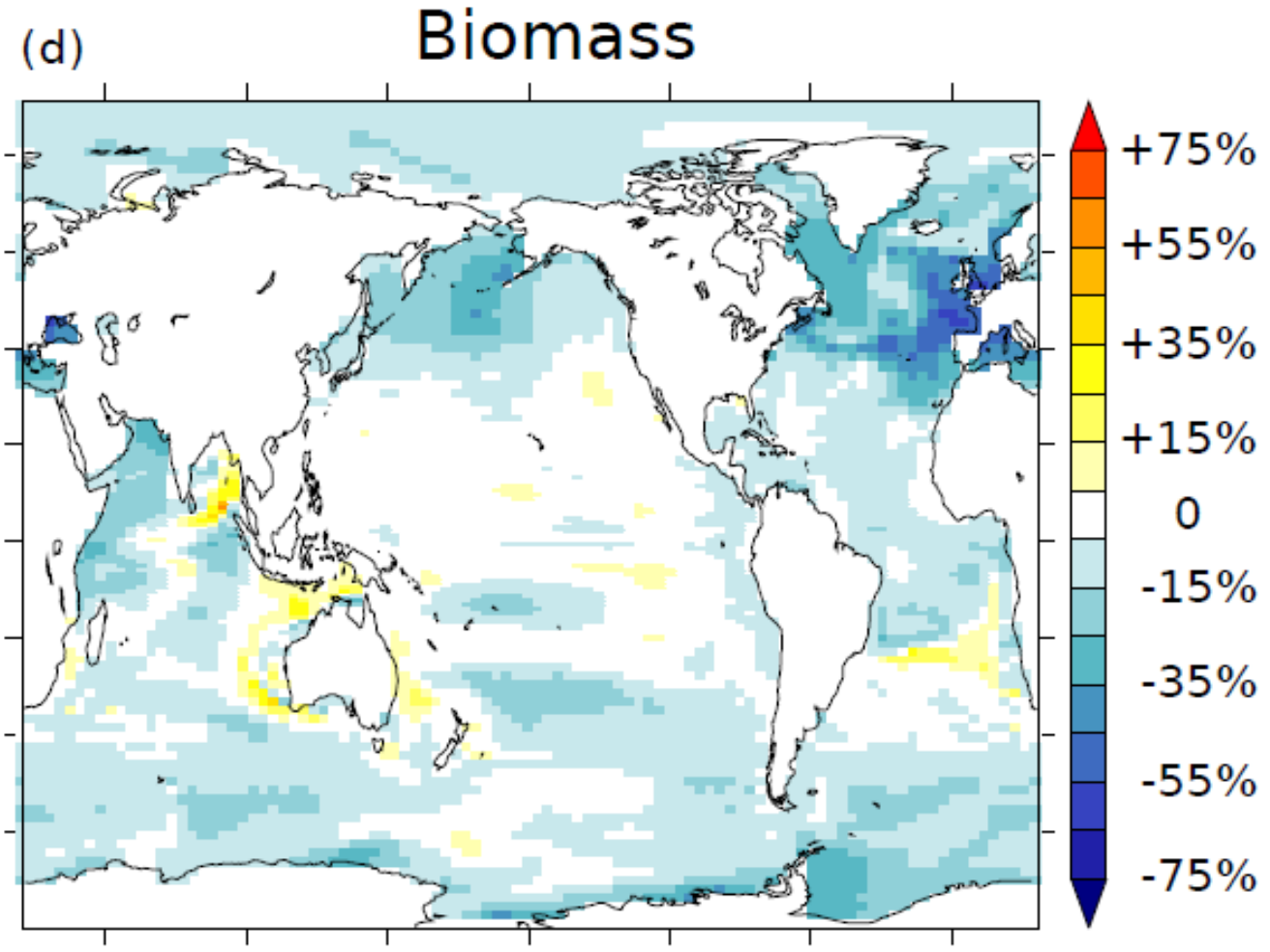

Change in biomass pool from preindustrial to ~2100
(IPCC SERS A2; function of nutrients; Steinacher et al. 2010)

Global Estimates of Seafloor Biomass

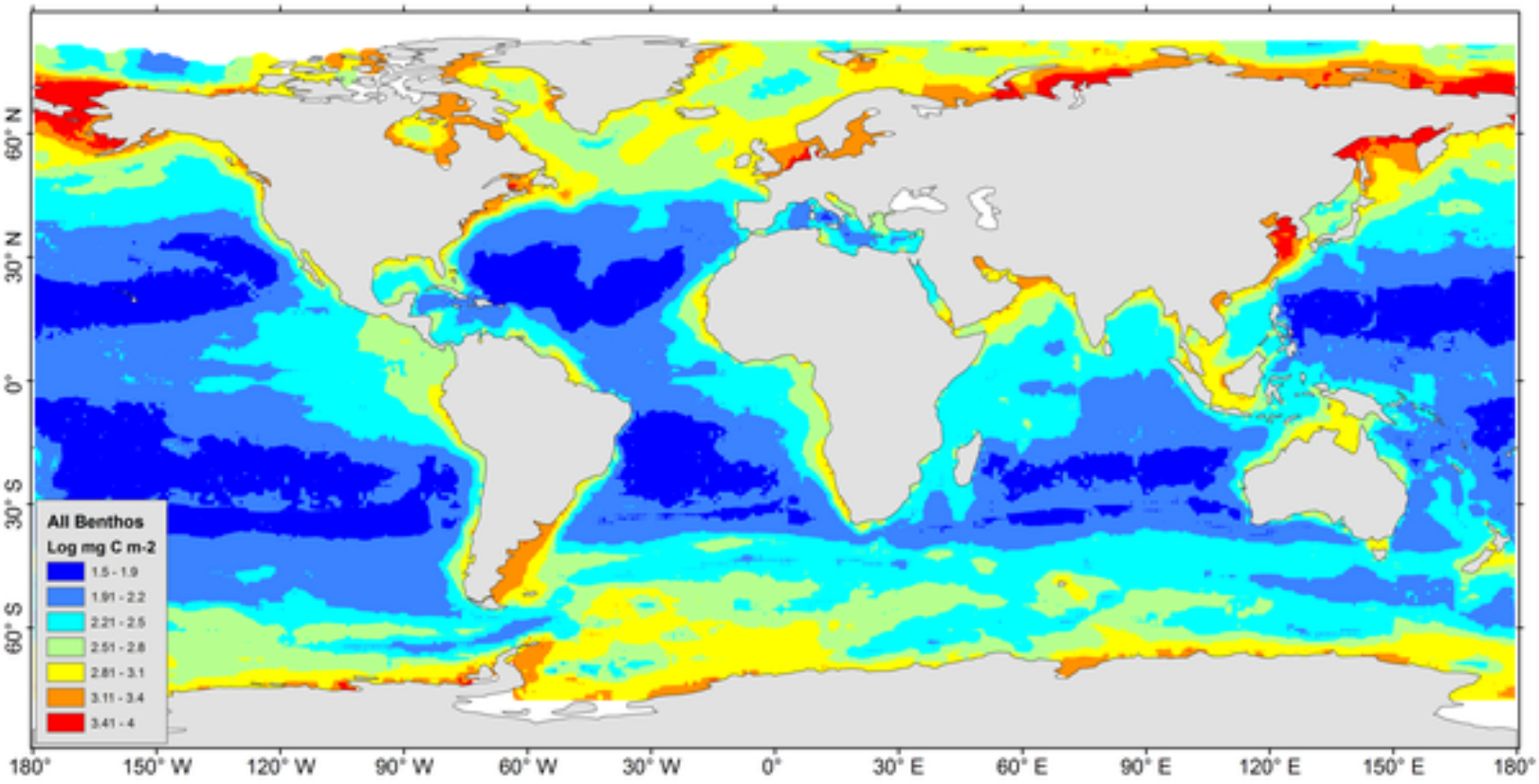

Established relationships between various parameters, including POC flux vs. Seafloor biomass
Wei et al., PLoS One, 2010

Global Estimates of Seafloor Biomass into the Future

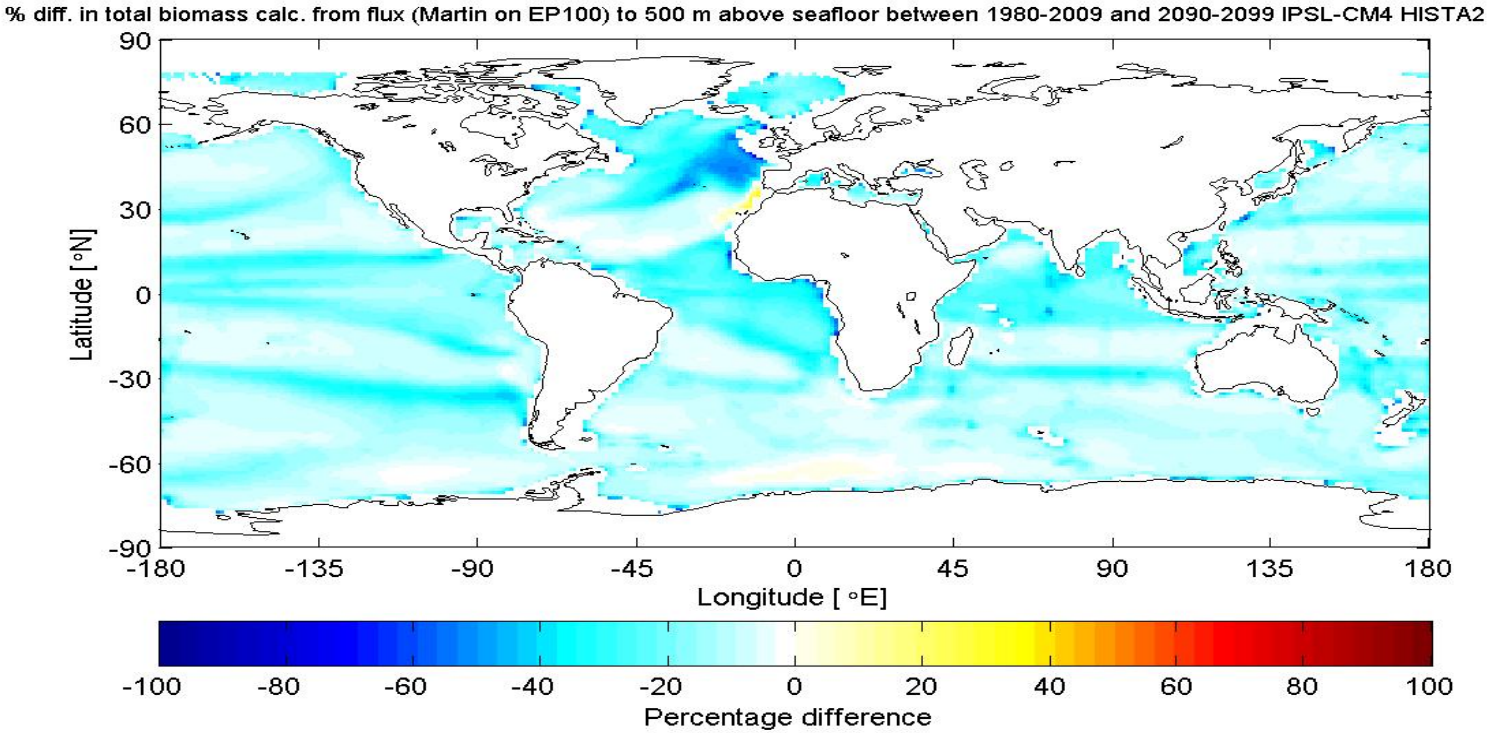

Jones, Ruhl et al., in prep

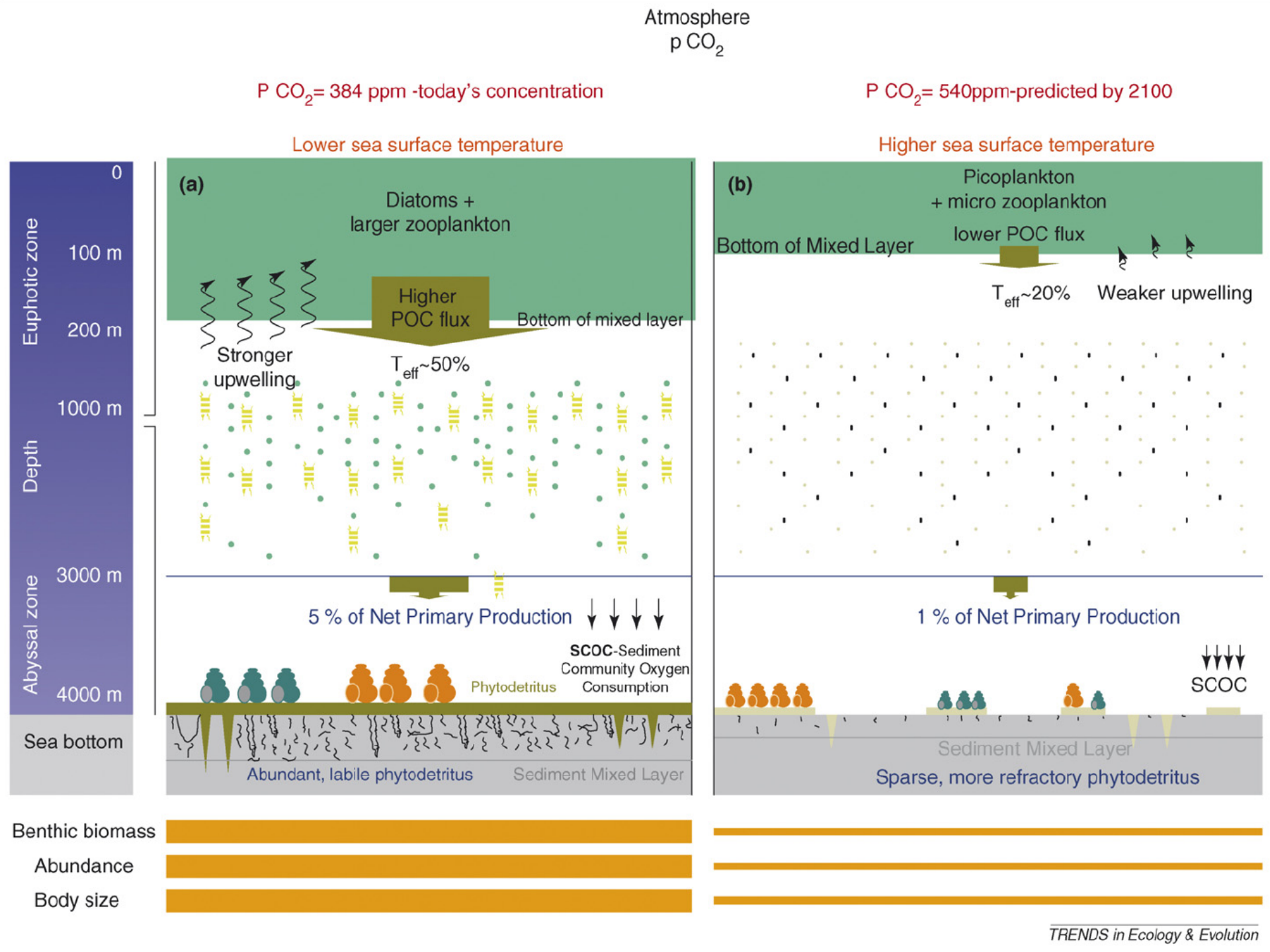
Atmosphere
p CO2
P CO2= 384 ppm -today's concentration
P CO2= 540ppm-predicted by 2100
Lower sea surface temperature
Higher sea surface temperature
0
Euphotic zone
100 m
200 m
Depth
1000 m
3000 m
Abyssal zone
4000 m
Sea bottom
(a)
Diatoms +
larger zooplankton
Higher
POC flux
Bottom of mixed layer
Stronger
upwelling
Teff~50%
5 % of Net Primary Production
SCOC-Sediment
Community Oxygen
Consumption
Phytodetritus
Abundant, labile phytodetritus
Sediment Mixed Layer
(b)
Picoplankton
+ micro zooplankton
Bottom of Mixed Layer
lower POC flux
Teff~20%
Weaker upwelling
1 % of Net Primary Production
SCOC
Sediment Mixed Layer
Sparse, more refractory phytodetritus
Benthic biomass
Abundance
Body size

Thanks for your attention!

Photo: A. Jamieson, Oceanlab, University of Aberdeen

National Oceanography Centre
NATURAL ENVIRONMENT RESEARCH COUNCIL

PAP Porcupine Abyssal Plain Observatory

Oceans 2025

NATURAL ENVIRONMENT RESEARCH COUNCIL

UNIVERSITY OF ABERDEEN

Oceanlab

Met Office

University of BRISTOL

University of Glasgow

NATURAL HISTORY MUSEUM

UNIVERSITY OF Southampton

Marine Institute
Foras na Mara

HERMIONE

EuroSITES
European Ocean Observatory Network

ESONET NOE

european multidisciplinary seafloor observatory
emso